A Hybrid Deterministic−Stochastic Algorithm for Modeling Cell Signaling Dynamics in Spatially Inhomogeneous Environments and under the Influence of External Fields

Dennis C. Wylie,[†,‡] Yuko Hori,[§] Aaron R. Dinner,[||] and Arup K. Chakraborty*,[⊥]

Biophysics Graduate Group and Departments of Chemistry and Physics, University of California, Berkeley, Berkeley, California 94720, Physical Biosciences Division, Lawrence Berkeley National Laboratory, Berkeley, California 94720, Department of Chemistry, University of Chicago, Chicago, Illinois 60637, and Departments of Chemical Engineering and Chemistry and Division of Biological Engineering, Massachusetts Institute of Technology, Cambridge, Massachusetts 02139

Received: October 28, 2005; In Final Form: March 13, 2006

Cell signaling dynamics mediate myriad processes in biology. It has become increasingly clear that inter- and intracellular signaling reactions often occur in a spatially inhomogeneous environment and that it is important to account for stochastic fluctuations of certain species involved in signaling reactions. The importance of these effects enhances the difficulty of gleaning mechanistic information from observations of a few experimental reporters and highlights the significance of synergistic experimental and computational studies. When both stochastic fluctuations and spatial inhomogeneity must be included in a model simultaneously, however, the resulting computational demands quickly become overwhelming. In many situations the failure of standard coarse-graining methods (i.e., ignoring spatial variation or stochastic fluctuations) when applied to *all* components of a complex system does not exclude the possibility of successfully applying such coarse-graining to *some* components of the system. Following this approach alleviates computational cost but requires "hybrid" algorithms where some variables are treated at a coarse-grained level while others are not. We present an efficient algorithm for simulation of stochastic, spatially inhomogeneous reaction−diffusion kinetics coupled to coarse-grained fields described by (stochastic or deterministic) partial differential equations (PDEs). The PDEs could represent mean-field descriptions of reactive species present in large copy numbers or evolution of hydrodynamic variables that influence signaling (e.g., membrane shape or cytoskeletal motion). We discuss the approximations made to derive our algorithm and test its efficacy by applying it to problems that include many features typical of realistic cell signaling processes.

1. Introduction

Signaling processes in cells play a key role in mediating biological functions.[1] Often, signaling is initiated by the binding of receptors expressed on the cell surface to a ligand present in solution or expressed on the surface of an apposing cell. This binding event can result in a series of biochemical reactions in the membrane-proximal region and the cytosol that can ultimately lead to upregulation of gene transcription factors and effector functions. Signaling processes and the activation of effector functions are emergent properties that result from cooperative dynamic events that involve many molecular components. The inherently cooperative nature of the pertinent dynamical processes makes it very difficult to intuit underlying mechanisms from observations of just a few experimental reporters.

Imaging data from a number of recent experiments, particularly those focused on signaling in T lymphocytes,[2−8] have produced vivid images that reveal a further complication. Many of the chemical reactions that are involved in signaling pathways occur in a spatially inhomogeneous environment. For example, various membrane proteins involved in signaling can be in a spatially organized pattern. A good example of this is provided by the immunological synapse, which is a specific spatial pattern of different proteins that forms in the intercellular junction between T lymphocytes and antigen-presenting cells when receptors and ligands expressed on these cells are engaged.[6,8,9] Intracellular proteins involved in signaling also organize into specific spatially organized structures. For example, scaffold proteins bind kinases involved in the MAPK signaling module in sequence, and this is important for many functions including the prevention of cross-talk between pathways.[10]

A mechanistic understanding of cell signaling processes therefore requires elucidation of collective dynamic processes that occur in a spatially inhomogeneous environment. Understanding these processes pertinent to cell signaling has been aided by synergy between theoretical and computational studies and genetic, biochemical, and imaging experiments.[3,7,11−14] We expect that this paradigm of combining computational modeling with experiments to develop a mechanistic understanding of cell signaling processes will continue to mature in the coming years. This will require the development of efficient computational algorithms that can simulate biochemical reactions that occur in a spatially inhomogeneous environment both on the plasma membrane and in the cytosol. One way to accomplish this is to use partial differential equations (PDEs) that model the pertinent reaction and transport processes. This is clearly a useful

* Author to whom correspondence should be addressed. E-mail: arupc@mit.edu.
[†] Biophysics Graduate Group, University of California, Berkeley.
[‡] Lawrence Berkeley National Laboratory
[§] Departments of Chemistry and Physics, University of California, Berkeley.
[||] University of Chicago.
[⊥] Massachusetts Institute of Technology.

10.1021/jp056231f CCC: $33.50
Published on Web 06/02/2006

approximation that can be very fruitful for studying certain problems. However, such a mean-field description becomes inappropriate for species that are present in low copy numbers. This is because fluctuations are important in this case, and one needs to solve the pertinent master equations.[15] It is worth remarking that stochastic fluctuations are even more important in a spatially inhomogeneous environment because the number of molecules in a given region is generally fewer than the total number of molecules in all regions, and the local value of this number is important.

Kinetic Monte Carlo algorithms[16] have been used to study stochastic cell signaling processes in a spatially inhomogeneous environment.[3,17] However, these methods are computationally intensive as many attempts to change the state of the system are rejected. Gillespie[18] devised a clever and more efficient algorithm to effectively solve chemical master equations, and his method has become a standard for stochastic dynamic simulations of chemical reactions that occur in a spatially homogeneous environment. An important modification of the Gillespie method is due to Elf et al.,[19] and this allows incorporation of the effects of spatial inhomogeneity.

The discrete fluctuating dynamic variables governing cell behavior are often influenced by variables that can be described by mean-field partial differential equations. Examples of such variables include concentration fields of molecular species that participate in signaling reactions, but are present in large numbers, and hydrodynamic variables such as the cell membrane shape and cytoskeletal motion that are known to be important during processes such as the recognition of antigen by T lymphocytes and subsequent signaling processes.[20−25]

In principle, the evolution of these variables could also be obtained by stochastic simulation. However, the enormous computational cost of treating all variables at this level of detail is unwarranted as it does not provide additional information compared to a method that could treat the appropriate variables stochastically and the others using field equations. Thus, there is a need for efficient hybrid algorithms wherein some variables are described by discrete dynamics and others evolve according to partial differential equations for continuous fields. At the spatially homogeneous level, such hybrid algorithms have been proposed.[26,27] Combining such hybrid approaches with spatial inhomogeneity introduces novel challenges with regard to the construction of efficient algorithms.

In this paper, we develop a stochastic method for simulating cell signaling in a spatially inhomogeneous environment where the discrete reaction dynamics of some molecular components is coupled to continuous fields that evolve according to partial differential equations. Our treatment of spatial heterogeneity in the context of the Gillespie algorithm is different from previous developments in that it is based on Gillespie's original "First Reaction Method" as opposed to the "Next Reaction Method" of Gibson et al.[28] but differs from both methods in that we keep track of simulation time in a novel manner by the addition of a "stochastic clock" reaction. This clock reaction reduces the number of random numbers that need to be generated during the simulation and in addition provides a convenient mechanism for handling the coupling of the evolution of discrete and continuous variables. The algorithm is described in section 2, and its strengths and weaknesses are discussed. In section 3, we compare the performance of two computational schemes proposed in section 2 by simulating two test problems. Here, we also compare the algorithm described in this paper to those that have been previously proposed. In section 4, we apply the method to simulate a complex biological problem, the recruitment of peptide−major histocompatibility complex (pMHC) molecules to the immunological synapse.[3,6,8,9,29] Finally, we offer brief concluding remarks. In three appendices, we describe some of the algebraically complicated derivations that lead to the equations that underlie the algorithm described in section 2 and certain details regarding the model systems that we simulate to compare these algorithms.

2. A Stochastic Algorithm for Spatially Inhomogeneous Reaction Dynamics

Gillespie developed a rigorous stochastic simulation algorithm for simulating the temporal evolution of a well-mixed system of reacting molecules.[18] The method can be viewed as a spatially homogeneous form of continuous time Monte Carlo[30] in which the population of each molecular species (k) is represented by a discrete number (n_k) and the time between events (τ) varies. Throughout the paper, a "molecular species" or "molecule" can refer to a single molecule or it can refer to a multimeric complex.

Defining the propensity of reaction $a(i,t)$ for the ith reaction at time t as the product of an intrinsic rate of reaction (i.e., a rate constant) and the values of n_k for the reactants involved, the probability that the ith reaction occurs during the infinitesimal time interval dt can be written as $a(i,t)\,\mathrm{d}t$. For example, if the ith reaction is the binding of two species A and B according to first-order kinetics, we have

$$a(i,t) = k_i n_A(t) n_B(t) \tag{1}$$

where k_i is the rate constant for the binding reaction, $n_A(t)$ is the number of A molecules at time t, and $n_B(t)$ is the number of B molecules at time t. Through the use of this propensity of reaction, the probability that the next reaction that will occur out of m distinct types is the ith one is given by

$$P(i,t) = \frac{a(i,t)}{a_{\mathrm{total}}(t)} \tag{2}$$

where

$$a_{\mathrm{total}}(t) = \sum_{j=1}^{m} a(j,t) \tag{3}$$

Assuming that the intervals between events (τ) follow the usual Poisson waiting time distribution

$$p(\tau)\,\mathrm{d}\tau = a_{\mathrm{total}} \exp(-a_{\mathrm{total}}\tau)\,\mathrm{d}\tau \tag{4}$$

with the time interval τ being

$$\tau(r) = -\left(\frac{\ln r}{a_{\mathrm{total}}}\right) \tag{5}$$

where r is a random number with probability distribution

$$P(r)\,\mathrm{d}r = \begin{cases} \mathrm{d}r & 0 < r < 1 \\ 0 & \text{otherwise} \end{cases} \tag{6}$$

This result derives from the transformation

$$p(\tau)\,\mathrm{d}\tau = P(r)\left|\frac{\mathrm{d}r}{\mathrm{d}\tau}\right|\mathrm{d}\tau = a_{\mathrm{total}} \exp(-a_{\mathrm{total}}\tau)\,\mathrm{d}\tau \tag{7}$$

The Gillespie algorithm is a clever scheme that utilizes two random numbers to generate states conforming to the distributions above (eqs 2 and 4). One random number determines the time between events (eq 5). A second random number deter-

mines which type of reaction occurs in that interval. In practice, the reaction that occurs (denoted μ) is selected with the weighting scheme in eq 2 by employing the relation

$$\sum_{j=1}^{\mu-1} a(j,t) < r' a_{\text{total}}(t) \leq \sum_{j=1}^{\mu} a(j,t) \tag{8}$$

where r' is a random number selected from a uniform distribution on the interval (0, 1).

An efficient variant of this algorithm has been developed that requires only a single random number per step.[28] The basic scheme is to generate a list of the stochastically generated times of next occurrence of each reaction type in the system and then iterate by performing the reaction with the lowest time of next occurrence. This is followed by updating the times of next occurrence of each reaction type according to a formula derived in Gibson et al.,[28] which does not require the generation of another random number for any reaction type other than the one just performed. Thus, the next reaction can be accurately chosen by again picking the lowest time in the list.

In the absence of external fields, we can use the algorithm reported in Elf et al.[19] to solve master equations corresponding to signaling reactions in a spatially inhomogeneous medium where molecular diffusion can also occur. The system is divided into N bins, of side length L, and molecular diffusion is treated by introducing hopping reactions that move molecules from one bin to a neighboring bin with rate constants given by D/L^2. (D is the diffusion constant of the molecular species in question.) The state of the system is defined by the number of molecules of each type in each bin, which we will denote by $\{n_k(\mathbf{x},t)\}$. The propensities of nonhopping reactions are also redefined to be local quantities, $a(i,\mathbf{x},t)$, where $\mathbf{x}$ denotes the location of a particular bin. Through the use of the local propensity of reaction, eqs 2 and 6 are modified as

$$P(i,\mathbf{x},t) = \frac{a(i,\mathbf{x},t)}{a_{\text{global}}(t)} \tag{9}$$

$$\tau(r) = -\left(\frac{\ln r}{a_{\text{global}}}\right) \tag{10}$$

where

$$a_{\text{global}}(t) = \sum_{\mathbf{y}} \sum_{j=1}^{m} a(j,\mathbf{y},t) \tag{11}$$

Here we follow Gillespie's First Reaction Method as opposed to Gibson's Next Reaction Method, used by Elf et al.,[19] and this will be discussed further below.

As we have noted earlier, in many systems (e.g., T lymphocytes), studying realistic cell signaling processes in a computationally tractable manner requires that a spatially inhomogeneous stochastic algorithm be coupled to the evolution of a set of continuous fields. For instance, consider the spatio-temporal evolution of a species (present in large copy number) described by a concentration field evolving according to a Fickian diffusion term as well as the discrete reaction events in which it participates. The equation that describes this process can be written as

$$\frac{\partial c(\mathbf{x},t)}{\partial t} = D\nabla^2 c(\mathbf{x},t) - \sum_{i=1}^{m} k_i(\mathbf{x},t) c(\mathbf{x},t) + \sum_{\mathbf{x}'} \delta(\mathbf{x}-\mathbf{x}') \sum_{i=1}^{m} S_i \sum_{j} \delta(t - t_{i,j}(\mathbf{x}')) \tag{12}$$

where S_i is the stoichiometric coefficient of the species described by the field c for the ith reaction. This equation is derived in Appendix 1 with a discussion of the relevant approximations. The primary approximations are that the species described by the field, c, diffuses very quickly on the length scale L of one bin and that the local concentration of this species is much greater than one particle per L^d (i.e., one particle per bin). Note that, in general, $a(i,\mathbf{x},t)$ now may depend not only on $\{n_k(\mathbf{x},t)\}$ but also on $\{c_l(\mathbf{x},t)\}$; i.e., the propensities for the discrete reaction events may depend on the distribution of the fields as well as the populations of the discrete species in each bin. Thus, the time evolution of the continuous fields and the discrete species are coupled. Equation 12 can be solved by standard finite difference methods. Each time a stochastic event (a reaction or a hop) takes place, we update discrete variables and evolve $c(\mathbf{x},t)$ according to eq 12 for the time τ obtained from eq 10. If τ is too large to obtain a numerically stable solution for eq 12, then we use a fixed time step Δt and repeatedly advance the associated clock by Δt up to a duration equal to τ. The field is then fixed, all propensities of reactions are updated to evolve the discrete molecular distributions further, and the cycle is repeated.

In principle, this extended algorithm allows us to simulate a spatially inhomogeneous stochastic reacting system coupled to deterministically evolving external fields. However, this scheme becomes computationally expensive for spatially large systems (many bins) with numerous possible reactions. There are two major difficulties: (1) proliferation of distinct types of reaction events (reaction events at distinct spatial bins are distinct types of reaction events) and (2) the enormous number of spatially distinct reactions makes the time between successive events in the whole system (τ) very small. This, in turn, makes the simulation of discrete events and the integration of the continuum equations over long times difficult. Below, we present methods that aim to alleviate these difficulties. In the next section, we will evaluate their relative efficacies.

Difficulty One: Gillespie Algorithm with Many Reactions. This difficulty can be highlighted without including a discussion of the coupling between discrete and continuous variables. The introduction of spatial heterogeneity dramatically increases the number of distinct reaction types. If in the spatially homogeneous description of the system there are M reaction types and Q species, then in the d-dimensional inhomogeneous description (divided into N spatial bins) there will be $R = N(M + 2dQ)$ distinct reaction types (after we include the hopping reactions representing diffusion and ignoring boundary effects). This problem appears in a slightly different form in the Next Reaction Method[28] and its spatially inhomogeneous form as proposed by Elf et al.[19] However, some of the computational techniques used to improve the efficiency of the Next Reaction Method have been translated into forms usable in the First Reaction Method as well[28] and will be discussed below.

In any given iteration of the Gillespie procedure, to decide which type of reaction event will occur next we generate a random number r in the range $(0, \sum_{\beta=1}^{R} a_\beta)$, where β indexes an enumeration of all R reaction types; we then perform reaction λ, where λ is determined by the condition that $r \in (\sum_{\beta=1}^{\lambda-1} a_\beta, \sum_{\beta=1}^{\lambda} a_\beta)$.

TABLE 1: Scheme 1 Applied to a System with $R = 7$ (i.e., 7 Reactions)

$N_{0,0} = 1$								$N_{0,1} = 7$
$N_{1,0} = 1$				$N_{1,1} = 4$				$N_{1,2} = 7$
				$S_{1,1} = a_1 + a_2 + a_3$				
$N_{2,0} = 1$		$N_{2,1} = 3$		$N_{2,2} = 4$		$N_{2,3} = 6$		$N_{2,4} = 7$
		$S_{2,1} = a_1 + a_2$				$S_{2,3} = a_4 + a_5$		
$N_{3,0} = 1$	$N_{3,1} = 2$	$N_{3,2} = 3$	$N_{3,3} = 4$	$N_{3,4} = 4$	$N_{3,5} = 5$	$N_{3,6} = 6$	$N_{3,7} = 7$	$N_{3,8} = 7$
	$S_{3,1} = a_1$		$S_{3,3} = a_3$		$S_{3,5} = a_4$		$S_{3,7} = a_6$	

If we know the partial sums $\sum_{\beta=1}^{n} a_\beta$ for all $n \in (1, R)$, then we can determine λ in $O(\lg R)$ steps by performing a recursive binary search for the correct interval. The basic idea is to divide the list of reactions into two blocks and compare the random number r to the sum of all of the quantities a_β in the first block to decide whether the reaction to be performed is in that block or the second. The chosen block is then divided in two again, and the process repeated iteratively until only one reaction remains in the last block. This is the reaction to be performed. However, the fact that the reaction propensities $a_\beta(t)$ are functions of time complicates matters because there is a dramatic increase in computational time if $O(R)$ values of these partial sums have to be recomputed each time we change some of the reaction propensities. We now discuss two schemes to alleviate this difficulty.

Scheme 1: Recursive Binary Search. This scheme is similar to the use of binary search trees described in Newman et al.[31] and one described in Gibson et al.[28] and applies some of the ideas they proposed in the context of the Next Reaction Method to the First Reaction Method of Gillespie.[18] The idea is essentially that described above, in that we compare the random number $r \in (0, \sum_{\beta=1}^{R} a_\beta)$ to partial sums of a_β to determine in which block of reactions the reaction to occur is located. The difference is that at each iteration of the search process, if r is greater than the appropriate partial sum (i.e., the reaction will be in the second of two reaction blocks as described above), then we subtract that partial sum from r before moving onto the next iteration. This results in having to keep track of partial sums of fewer of the a_β values. Hence, fewer partial sums must be updated as a result of any one a_β changing. To accomplish this, the following procedure must be followed.

We define the following quantities, where $\lceil u \rceil$ indicates the lowest integer greater than u, $\lfloor u \rfloor$ indicates the largest integer less than u, and lg refers to $\log_2$:

(1) Define $c = \lceil \lg R \rceil$, $N_{0,0} = 1$, and $N_{0,1} = R$ where R is again the number of reactions. Then for every integer i between 1 and c (inclusive), define also

(2) For each even integer j from 0 to 2^i, $N_{i,j} = N_{i-1,j/2}$.

For each odd j in the range from 0 to 2^i, $N_{i,j} = \lceil (N_{i-1,(j+1)/2} - N_{i-1,(j-1)/2})/2 \rceil + N_{i-1,(j-1)/2}$.

(3) For each odd j from 0 to 2^i, $S_{i,j}(t) = \sum_{\beta=N_{i-1,(j-1)/2}}^{N_{i,j}-1} a_\beta(t)$. (Note that the two-index quantities $S_{i,j}$ defined here are unrelated to the stoichiometric coefficients S_i in eq 12.) The quantities $N_{i,j}$ define the boundaries of the blocks into which the reactions are partitioned as described above, while the quantities $S_{i,j}$ are the corresponding partial sums of the quantities a_β. Note that unlike $N_{i,j}$, $S_{i,j} = S_{i,j}(t)$ must be updated every time one of the a_β in the appropriate summation range changes. However, any given a_β is only in the summation range of $O(\lg R)$ distinct $S_{i,j}$ values. This fact is the motivation for this particular scheme involving $N_{i,j}$ and $S_{i,j}$.

In any given iteration of the algorithm, we decide which reaction should occur with the aid of the random number, r, generated using the scheme described above. The following steps are then executed:

(1) Begin by setting $i = j = 1$.

(2) If $r \le S_{i,j}$, reset $i \rightarrow i + 1$, $j \rightarrow 2j - 1$.

If $r > S_{i,j}$, reset $i \rightarrow i + 1$, $j \rightarrow 2j + 1$, $r \rightarrow r - S_{i,j}(t)$.

(3) If $i < c$, repeat step 2. Otherwise, if $r \le S_{c,j}$, perform reaction $(N_{c,j} - 1)$, while if $r > S_{i,j}$, perform reaction $N_{c,j}$.

Thus, by keeping track of certain sums of reaction propensities we can quickly deduce which reaction should occur next. Consider the following example for a system with $R = 7$ reactions (Table 1) (in this case, $c = 3$). If the random number that is picked, r_0, lies in the range $(\sum_{\beta=1}^{4} a_\beta, \sum_{\beta=1}^{5} a_\beta)$, say $r_0 = z + \sum_{\beta=1}^{4} a_\beta$ where $0 < z < a_5$, we would follow the algorithm as follows:

(i) $r_0 = (z + \sum_{\beta=1}^{4} a_\beta) > \sum_{\beta=1}^{3} a_\beta = S_{1,1} \rightarrow$ set $i = 2$, $j = 2 \times 1 + 1 = 3$, and $r = r_0 - S_{1,1} = z + a_4$

(ii) $r = (r_0 - S_{1,1}) = (z + a_4) < (a_4 + a_5) = S_{2,3} \rightarrow$ set $i = 3$ and $j = 2 \times 3 - 1 = 5$

(iii) $r = (z + a_4) > a_4 = S_{3,5} \rightarrow$ perform reaction $N_{3,5} = 5$

The essential idea of the approach embodied in Scheme 1 above is the use of a recursive binary search of the list of reactions to deduce which reaction to do next. While this greatly reduces the amount of time required to decide what the next event should be in each iteration, it increases the number of computations that must be performed to update the reaction propensities. This is because we must also update all of the associated sums, $S_{i,j}$. By breaking the search task inherent in making the next reaction decision down into blocks of more than two elements at each of the i iterations described above (i.e., replacing the "recursive binary search" with a "recursive n-ary search" for some $n > 2$), a balance can be struck between the time required for each of these two computational tasks. While the amount of time required to locate the appropriate next reaction increases as n increases, there is an associated decrease in the number of quantities $S_{i,j}$ that must be computed. In general, a recursive n-ary search scheme would require updating $\lceil \log_n R \rceil$ quantities each time a reaction propensity is updated. However, locating the correct next reaction (given r) will require $O((n-1)\lceil \log_n R \rceil)$ comparisons of r with various sums of reaction propensities $S_{i,j}^{(n)}$. The optimal choice of n for such a scheme depends on the average number of reaction propensities that must be updated in each iteration of the procedure.

Scheme 2: Coordinate Decomposition Search Scheme. The number of blocks (n) of reaction propensity sums that need to be compared to r need not be a constant in each iteration. If we have an obvious decomposition of reactions into blocks we might choose to have n vary from one iteration to the next according to the size of the blocks in question. For instance, for a spatially homogeneous code in two spatial dimensions (x,y), we could use the following scheme (Scheme 2):

(1) Keep track of the cumulative sums of reaction propensities in each bin separately; that is, define

$$a_{\text{local}}(\mathbf{x},t) = \sum_i a(i,\mathbf{x},t)$$

(2) Keep track also of sums of reaction rates of all reactions in coordinate slices defined by y (= constant); that is

$$b_{\text{slice}}(y,t) = \sum_{i,x} a(i,x,y,t) = \sum_{x} a_{\text{local}}(x,y,t)$$

(3) Given a random number, r, determine which reaction occurs next by sequentially determining y, then x, then i, according to the conditions

$$\text{(3a) } y \text{ must satisfy: } \quad r \in \left(\sum_{y'=0}^{y'=y-L} b_{\text{slice}}(y',t), \sum_{y'=0}^{y'=y} b_{\text{slice}}(y',t) \right)$$

(3b) x must satisfy:

$$\left(r - \sum_{y'=0}^{y'=y-L} b_{\text{slice}}(y',t) \right) \in \left(\sum_{x'=0}^{x'=x-L} a_{\text{local}}(x',y,t), \sum_{x'=0}^{x'=x} a_{\text{local}}(x',y,t) \right)$$

(3c) i must satisfy:

$$\left(r - \sum_{y'=0}^{y'=y-L} b_{\text{slice}}(y',t) - \sum_{x'=0}^{x'=x-L} a_{\text{local}}(x',y,t) \right) \in \left(\sum_{i'=0}^{i'=i-1} a(i',x,y,t), \sum_{i'=0}^{i'=i} a(i',x,y,t) \right)$$

In this scheme, whenever we update the reaction rate $a(i,x,y,t)$, we must only update $a_{\text{local}}(x,y,t)$, $b_{\text{slice}}(y,t)$, and the sum of all reaction propensities, which determines the upper bound on r for the next reaction event. However, if the numbers of horizontal and vertical bins are very large or if the number of reactions in each bin is large, then this scheme may be less efficient than Scheme 1 as a result of the many comparisons that must be made in finding (y,x,i) that satisfy the conditions in step 3 above.

Difficulty Two: Elapsed Time and the Stochastic Clock. The stochastically determined time interval between consecutive reaction events in our system is generally much smaller than the precision with which we need to keep track of time. We have two interests in keeping track of time: (1) We need to know, to within some error range, how much time has passed since the beginning of the simulation, and (2) we need to know when enough time has passed for us to call on the finite difference algorithm that updates the continuous field variables. In the discussion below, we assume that the time step used to integrate the continuous field equations is smaller than the error range within which we need to keep track of the elapsed time, τ, since the beginning of the simulation.

Thus, we seek to avoid updating time every time a reaction occurs, as called for by Gillespie's original procedure. Instead, we update time only as required for accurate integration of the field equations. We describe a procedure for doing this, the "Stochastic Clock Method" below.

We introduce a "clock bin" that is decoupled from the rest of the bins and in which the only "reaction" that can occur is the passage of time. The propensity of this zeroth-order time advancement reaction remains constant during the simulation

$$a_{\text{clock}}(\mathbf{x}_c,t) = \Gamma \tag{13}$$

where subscript c denotes the clock bin. We now seek to find the probability distribution of the interval τ between two successive time clock advancement events ("clock ticks") given a particular sequence of reaction events occurring in that interval.

Set time 0 at the last clock tick. Define $b_1 = a_{\text{global}}(0)$ as the sum of all reaction rates (including the clock tick rate a_{clock}) in the system at time 0. Let t_1 be the time of the next reaction (which we assume is not a clock tick). Then

$$p(t_1) = b_1 \exp[-b_1 t_1] \tag{14}$$

Now define $b_2 = a_{\text{global}}(t_1)$ as the sum of all reaction rates immediately after whatever reaction was chosen to occur at t_1. The time elapsed between t_1 and the next reaction after t_1 is a random variable t_2, independent of t_1, distributed according to the formula

$$p(t_2) = b_2 \exp[-b_2 t_2] \tag{15}$$

We continue in this manner until, on the qth iteration, we happen to pick the clock-ticking reaction. The total time since the last clock tick is then $\tau = t_1 + t_2 + \cdots + t_q$, and for each i, we have

$$P(t_i) = b_i \exp(-b_i t_i) \rightarrow \langle\langle (t_i)^m \rangle\rangle = (m-1)!(b_i)^{-m} \tag{16}$$

Since the t_i values are all independent random variables, their sum (the total time since last clock tick) has cumulants equal to the sum of the cumulants of t_i; that is

$$\langle\langle \tau^m \rangle\rangle = \left\langle\left\langle \left(\sum_{i=1}^{q} t_i \right)^m \right\rangle\right\rangle = \sum_{i=1}^{q} \langle\langle (t_i)^m \rangle\rangle = \sum_{i=1}^{q} (m-1)!(b_i)^{-m} \tag{17}$$

The number of reactions q that have occurred since the clock tick at time 0 will generally be a large number assuming that the clock tick rate is small compared to the sum of all reaction rates in the system. (If it is not, then using the stochastic clock algorithm is irrelevant as it would be more efficient to keep track of time between any two consecutive reactions as per the standard Gillespie method.[18]) Thus we argue in the vein of the central limit theorem that the distribution for the time τ passed between clock ticks is well approximated by a Gaussian distribution with the same mean and variance. From the above, we know the mean and variance of τ

$$\langle \tau \rangle = \sum_{i=1}^{q} \frac{1}{b_i}$$
$$\langle\langle \tau^2 \rangle\rangle = \sum_{i=1}^{q} \frac{1}{(b_i)^2} \tag{18}$$

Thus we choose the stochastic clock-ticking reaction in exactly the same manner as any other reaction, but now, instead of updating the clock time t after every reaction event, we do so only when the reaction was the clock tick reaction. Also, the formula that we use to determine the amount by which to update the clock time is altered to

$$\tau = \sum_{i=1}^{q} \frac{1}{b_i} + \sqrt{\sum_{i=1}^{q} \frac{1}{(b_i)^2}}\, r_{\text{Gauss}} \tag{19}$$

where r_{Gauss} is a Gaussian random number with zero mean and unit variance.

During the interval τ, we evolve the state of the discrete part of the system as described above, making no change to the elapsed time of the system. It should be emphasized that, assuming the rate of clock ticking is much lower than the sum

of all other reaction propensities in the system, in following this procedure we are essentially drawing only one random number per iteration (which we use to decide what the next reaction will be)—only for those rare reaction events that are clock ticks do we need a second random number to decide how much time has passed. This manner in which we have reduced the number of calls to the random number generator per iteration is, however, quite different from that of the Next Reaction Method.[28]

When coupling this stochastic method to some set of continuous fields that evolve according to partial differential equations (e.g., eq 12), clock ticking also tells us when to update the field configurations. Each time the clock ticks (and only when the clock ticks), we advance the field equations by the stochastic interval τ. The numerical stability of the solution is enforced by adjusting the reaction rate Γ in eq 19, which may be set independently of any other time scale in the system. Note that while the probability distribution for the time τ between clock ticks (given a particular reaction sequence in the time interval) is dependent on all of the reaction rates in the system the probability distribution for τ over the ensemble of all possible sequences of reaction events between clock ticks depends only on the decoupled clock tick rate, Γ, and is given by

$$P(\tau) = \Gamma \exp(-\Gamma\tau) \tag{20}$$

Thus, if we want our average finite difference time step to be Δt, then we choose $\Gamma = (\Delta t)^{-1}$, independent of any other aspects of the system.

It should be mentioned that Salis et al.[27] have derived a hybrid stochastic method that approximates the evolution of fast reactions in a master equation by a chemical Langevin equation coupled to a modified Gillespie algorithm for slow reactions. This method could also be applied in a spatially inhomogeneous context with fast diffusive hopping reactions. This would replace the discrete stochastic hops from bin to neighboring bin with continuous, but still stochastic, transfer of (now, generally, noninteger-valued) numbers of particles according to the appropriate chemical Langevin equation. If, further, the fluctuation term in the chemical Langevin equation were ignored, such that only the deterministic part of the equation remained, the resulting algorithm would provide a way to couple the remaining deterministic continuum equations for the fast variables to the stochastic simulation of the discrete master equation for the slow variables. This scheme would effectively solve the same equations (if a stochastic PDE representing fields other than chemical species, like cell membrane shape fluctuations, were also included) as the technique described above. However, the underlying algorithm would be different; Salis et al.[27] put forward a simulation method based on advancing the state of the system by fixed time steps, in which the continuum equations are advanced by finite difference methods and a formula is applied to check whether a slow reaction happens during the time interval or not. (If a slow reaction does occur, then they also provide a way to determine when exactly in the time interval it occurred and to "rewind" the system to that point for further evolution.) In contrast, the method described above extends the First Reaction Method by including the finite difference step in the list of reactions and assigning it a reaction propensity inversely proportional to the mean finite difference time step desired.

It is a point worth mentioning that in simulating spatially inhomogeneous systems of large spatial extent (i.e., many bins) the issue of what is a fast or slow reaction is complicated by the presence of two time scales for each reaction: one associated with the time between reactions in a particular bin and another concerned with the time between reactions in the entire system. Reaction A may be much faster than reaction B, and yet between two successive occurrences of reaction A in a fixed bin **x** there may be many occurrences of reaction B in various bins elsewhere in the system. This is one of the motivating factors for extending the First Reaction Method in this paper: We want to treat fast-diffusing species by continuum methods, yet despite the relative quickness of these diffusion steps, there may be many occurrences of relatively "slow" reactions at various locations in the system (though the chance of occurrence of said slow reactions in any one bin may be small) over the time scales in which the continuum equations evolve appreciably.

It should also be noted that the Gillespie—Gibson Next Reaction Method can also be coupled to the integration of differential equations describing continuous fields.[26] This has been done only for ordinary differential equations (ODEs), but the extension to PDEs is straightforward, though for the spatially inhomogeneous models leading to PDEs we would need a spatially inhomogeneous variant of the Next Reaction Method along the lines of Elf et al.[19] The key to this approach is to note that the times at which we wish to call the finite difference routines can be added directly into the list of "next occurrence times" that the Gillespie—Gibson—Elf algorithm uses to determine what to do in each iteration. Then, when the lowest time in the list is the time associated with integrating the finite difference equations, we update the field configurations, adjust the propensities of all other reaction events as well as their associated next occurrence times, and then start the next iteration of the procedure. We compare the performance of such an extension of the Elf et al.[19] algorithm to the stochastic clock algorithm developed herein below.

TABLE 2: Small System Species Parameters for Time Tests of Schemes 1 and 2[a]

species	N_0	diffusion constant	z_i	λ_i	bias
L	200 000	1 $\mu m^2 s^{-1}$	N/A	N/A	N/A
I	20 000	1 $\mu m^2 s^{-1}$	N/A	N/A	N/A
LI	0	0.01 $\mu m^2 s^{-1}$	40 nm	50 kT μm^{-2}	N/A

[a] Note that for small system simulations all species were treated discretely. (The only field present is the membrane field.)

TABLE 3: Small System Reaction Network for Time Tests of Schemes 1 and 2

reaction	rate constant	Z_i	σ_i	cutoff
L + I → LI	0.33 $\mu m^2 s^{-1}$	40 nm	5 nm	5 nm
LI → L + I	0.1 s^{-1}	N/A	N/A	N/A

3. Relative Efficiency of the Different Computational Algorithms

We compare the methods presented in section 2 by applying them to simulate two different systems. These systems are models, which will be referred to below as the "small system", described in Tables 2—3, and the "large system", described in Tables 4—6.

The small system consists of two species, labeled L and I, which are embedded in two apposed cell membranes. L and I can bind to each other when they are opposite each other across the two membranes and in this sense represent a receptor and its ligand. The resulting complex also dissociates with a certain rate. The kinetics of the binding reaction depends on the intermembrane separation. This is because the complex, LI, formed upon binding has a preferred bond length. When the membranes are separated by a distance different from this bond

TABLE 4: Large System Species Abbreviations

L	LFA
I	ICAM
LI	LFA−ICAM complex
E	endogenous pMHC
A	agonist pMHC
M	pMHC (agonist or endogenous)
T	TCR
C	$(CD4-Lck)_2$ dimer
MT	pMHC−TCR complex
MTC	(pMHC−TCR)−$(CD4-Lck)_2$ complex
MTC′	stabilized (pMHC−TCR)−$(CD4-Lck)_2$ complex
MTCM	(pMHC−TCR)−$(CD4-Lck)_2$−pMHC complex
MTC′M	stabilized (pMHC−TCR)−$(CD4-Lck)_2$−pMHC complex
MTCMT	(pMHC−TCR)−$(CD4-Lck)_2$−(pMHC−TCR) complex
MTC′MT	stabilized (pMHC−TCR)−$(CD4-Lck)_2$−(pMHC−TCR) complex

TABLE 5: Large System Species Parameters

species	N_0	diffusion constant	z_i	λ_i	bias[a]
L[b]	200 000	1 $\mu m^2\ s^{-1}$	N/A	N/A	N/A
T[c]	100 000	1 $\mu m^2\ s^{-1}$	N/A	N/A	0.57 $\mu m\ s^{-1}$
C[b]	100 000	1 $\mu m^2\ s^{-1}$	N/A	N/A	N/A
I	20 000	1 $\mu m^2\ s^{-1}$	N/A	N/A	N/A
LI	0	0.01 $\mu m^2\ s^{-1}$	40 nm	50 kT μm^{-2}	N/A
M = E	30 000	1 $\mu m^2\ s^{-1}$	N/A	N/A	N/A
M = A	10	1 $\mu m^2\ s^{-1}$	N/A	N/A	N/A
MT	0	0.01 $\mu m^2\ s^{-1}$	15 nm	250 kT μm^{-2}	0.0057 $\mu m\ s^{-1}$
MTC	0	0.01 $\mu m^2\ s^{-1}$	15 nm	250 kT μm^{-2}	0.0057 $\mu m\ s^{-1}$
MTCM	0	0.01 $\mu m^2\ s^{-1}$	15 nm	250 kT μm^{-2}	0.0057 $\mu m\ s^{-1}$
MTCMT	0	0.01 $\mu m^2\ s^{-1}$	15 nm	250 kT μm^{-2}	0.0057 $\mu m\ s^{-1}$
MTC′	0	0.01 $\mu m^2\ s^{-1}$	15 nm	250 kT μm^{-2}	0.0057 $\mu m\ s^{-1}$
MTC′M	0	0.01 $\mu m^2\ s^{-1}$	15 nm	250 kT μm^{-2}	0.0057 $\mu m\ s^{-1}$
MTC′MT	0	0.01 $\mu m^2\ s^{-1}$	15 nm	250 kT μm^{-2}	0.0057 $\mu m\ s^{-1}$

[a] When present. [b] Treated as a field for all simulations other than time comparisons between Schemes 1 and 2. [c] As above, except also treated discretely for those simulations with a convective bias term in motion.

TABLE 6: Large System Reaction Network[a]

reaction	rate constant	Z_0	σ	cutoff
L + I → LI	0.33 $\mu m^2\ s^{-1}$	40 nm	5 nm	5 nm
LI → L + I	0.1 s^{-1}	N/A	N/A	N/A
M + T → MT	0.125 $\mu m^2\ s^{-1}$	15 nm	13.75 nm	5 nm
MTCM + T → MTC′MT	0.125 $\mu m^2\ s^{-1}$	15 nm	13.75 nm	5 nm
ET → E + T	1000 s^{-1}	N/A	N/A	N/A
ETC → E + T + C	1000 s^{-1}	N/A	N/A	N/A
AT → A + T	0.054 s^{-1}	N/A	N/A	N/A
ATC → A + T + C	0.054 s^{-1}	N/A	N/A	N/A
MT + C → MTC	0.125 $\mu m^2\ s^{-1}$	15 nm	13.75 nm	5 nm
MTC + M → MTCM	0.125 $\mu m^2\ s^{-1}$	15 nm	13.75 nm	5 nm
MTC′ + M → MTC′M	1.25 $\mu m^2\ s^{-1}$	15 nm	13.75 nm	5 nm
MTC → MT + C	0.02 s^{-1}	N/A	N/A	N/A
MTCM → MT + C + M	0.02 s^{-1}	N/A	N/A	N/A
MTC′ → MT + C	0.02 s^{-1}	N/A	N/A	N/A
MTC′M → MT + C + M	0.02 s^{-1}	N/A	N/A	N/A
MTCM → MTC + M	10 s^{-1}	N/A	N/A	N/A
MTC′M → MTC′ + M	10 s^{-1}	N/A	N/A	N/A
MTC′MT → MTC′ + MT	10 s^{-1}	N/A	N/A	N/A

[a] Note that in the simulations allowing for a convective bias in TCR diffusion (cytoskeletal motion), an additional set of phosphorylation and dephosphorylation reactions is present. Any species in the above containing a "T" bound to (i.e., written adjacent to) an "M" undergoes a first-order phosphorylation reaction with rate constant of 10 s^{-1}. A "T" can be phosphorylated only once. Phosphate groups are removed by a set of local zeroth-order reactions (one per 250 nm × 250 nm bin) with rate of 0.1 s^{-1}.

length, the probability of a reaction event is smaller (and so is the rate coefficient). A particular form of the dependence of the rate coefficient on the intermembrane separation must be chosen, and in Appendix 3 we describe the one that we use to carry out simulations herein. The choice is motivated by studies that are relevant to the formation of the immunological synapse between T lymphocytes and antigen-presenting cells.[6,8,22] The dependence of the rate coefficient on intermembrane separation is a simple way in which the discrete binding and unbinding events (of L and I) are coupled to a continuous field, the shape of the membrane. In the model that we simulate, the membrane shape evolves according to a time-dependent Landau−Ginzburg equation,[32] i.e., a stochastic partial differential equation. This requires us to formulate a free energy functional for the membrane shape. The free energy has contributions from three physical effects. Membrane shape changes that result in an increase in area are inhibited by a finite interfacial tension, high curvature shapes are not favored because of a finite bending rigidity, and membrane shape changes that extend or compress any LI bonds away from their preferred lengths are not favorable. The detailed free energy functional is provided in Appendix 3. Systems that require the incorporation of other continuous fields, such as cytoskeletal motion, can also be easily simulated using our algorithm, as we show in the next section. Tables 2−3 provide details on parameters used to carry out the simulations for the small system.

The large system is a model for membrane-proximal signaling initiated by the binding of a receptor to its cognate ligand as well as adhesion molecules that bind across two juxtaposed cells. Two kinds of ligands are present, one that binds weakly to the receptor and the other that binds more strongly. Receptor−ligand pairs as well as the two complementary adhesion molecules have preferred bond lengths, and hence, their rates of binding are coupled to intermembrane shape (continuous field) as in the small system described above. Also incorporated into the large system are certain cooperative mechanisms via which signaling due to the binding of the receptor to small amounts of strongly binding ligand is amplified by the weaker binding ligand. This amplification involves a membrane protein whose cytoplasmic tail carries a kinase (C) that can phosphorylate the receptor (T) when it is bound to a ligand (M). This model (Tables 4−6) is a simplified description of models that have been developed to study how T lymphocytes detect small amounts of antigen on the surfaces of antigen-presenting cells.[5,7,29] Tables 4−6 describe how the labels on the species relate to signaling events in T cells, and this connection will be elaborated in the next section. For the moment, this model represents a larger signaling system where the discrete binding events and membrane-proximal signaling are coupled to a continuous field, and we use it to compare the relative efficacy of various algorithms.

The small system was used to compare the two schemes presented in section 2. All our simulations use the stochastic clock described in section 2. An AMD Athlon XP 2000+ 1.26 GHz computer was used to compute dynamic trajectories of the system resulting from simulations with the two algorithms (Figure 1). All the computational times reported below are for simulating 1 s of real time for the large and small systems. The wall time taken for simulating a single trajectory of the small system was similar for the two schemes (407 ± 6 s for Scheme 1 and 289 ± 1 s for Scheme 2), with Scheme 2 showing a slight advantage.

The better performance of Scheme 2 compared to Scheme 1 indicates that the recursive binary search strategy of Scheme 1 can sometimes be improved on by something like a recursive *n*-ary search procedure. It should be noted that for a more complex system than the small system used to obtain these results (i.e., one for which more reaction propensities would have to be updated as a result of a reaction occurring) the recursive binary search of Scheme 1 will fare even worse relative

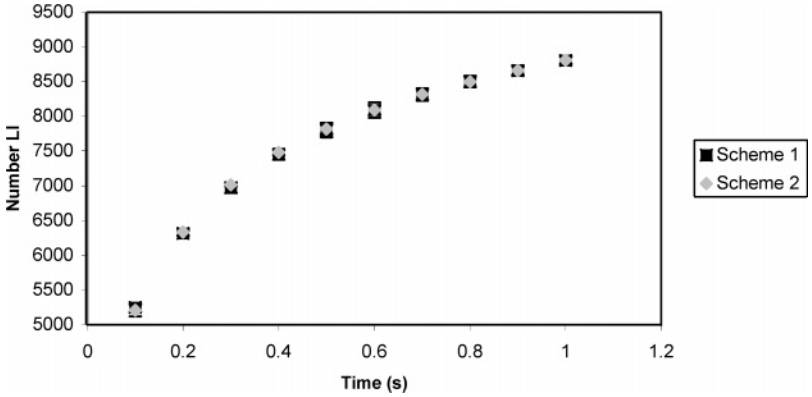

Figure 1. Trajectories obtained from Schemes 1 and 2 described in section 2 leading to equally accurate results for the average number of LI bonds. These results are for the small system.

to the recursive *n*-ary search of Scheme 2. This is demonstrated by simulation of the larger system described in Tables 4−6; the results of these simulations show a greater advantage in efficiency for Scheme 2 over Scheme 1 (wall time 1770 ± 40 s for Scheme 1 versus 710 ± 15 s for Scheme 2 for simulating a single trajectory) compared to that reported above for the smaller system.

Finally, we also simulated the large system using a variant of the Elf et al.[19] algorithm where the PDEs were coupled to the master equation in a manner similar to that used by Takahashi et al.[26] to couple ODEs to the spatially homogeneous Gillespie algorithm. Details of the simulation setup are shown in Tables 4−6. The stochastic clock algorithm was also used to simulate the same system for comparison. The wall time for the stochastic clock algorithm (Scheme 2) to simulate a single trajectory was 440 ± 20 s, while for the modified Elf et al. algorithm the wall time for the simulations was 900 ± 25 s. (For the simulations discussed in this paragraph only, a 2.20 GHz AMD Athlon XP 3200+ computer was used.)

This difference can be explained in light of the fact that the efficiency of the modified Elf et al. algorithm depends critically on the assumption that the reaction rates (and hence the time of next reaction occurrence) must be changed in at most two spatial bins per reaction/diffusion iteration; e.g., the bin in which a reaction occurred or the two bins involved in a diffusive hopping event. However, when the master equation is coupled to PDEs, we must alter the reaction rates in every spatial bin each time we update the field variables. The Elf et al. algorithm relies on maintaining an "event queue" containing the next reaction times of each bin in an ordered data structure allowing rapid determination of which bin has the lowest next reaction time at each iteration. If only one or two bins must be shuffled around in each iteration to maintain the ordering of the event queue, then the algorithm is very efficient. However, if the entire queue needs to be reordered very frequently (as is the case when reaction rates are changing in every bin as a result of updating the field variables in the modified Elf et al. algorithm above), then the efficiency is compromised.

4. Application to Signaling in T Lymphocytes

To further demonstrate the applicability of the more efficient algorithm described above, we study a problem concerned with signaling in T lymphocytes (T cells) that includes many features common to cell signaling processes. T cells are the orchestrators of the adaptive immune response. They are activated in response to the protein components of antigens. Peptides (p's) derived from antigenic proteins can bind to the products of the major histocompatibility complex (MHC), and these pMHC molecules

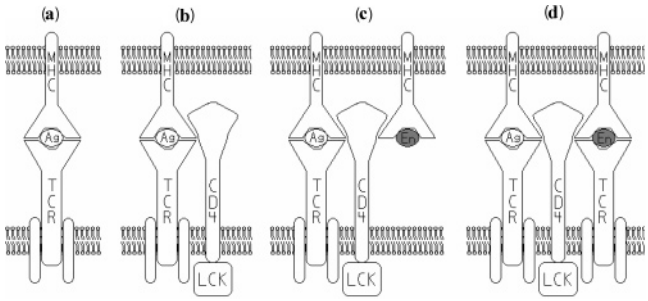

Figure 2. Membrane-proximal signaling showing cooperativity between agonist (Ag) and endogenous (En) pMHC molecules in triggering TCR. Lck is the kinase attached to the coreceptor (CD4) that phosphorylates the cytoplasmic domains of TCR. The cartoons do not represent molecular details of how the additional pMHC molecule associates with the signaling complex nucleated by Ag pMHC binding to TCR.

(designated as M in Tables 4−6) expressed on the surfaces of antigen-presenting cells (APCs) are the molecular signatures of antigens. T cell receptors (TCRs), designated as T in Tables 4−6, can bind to these pMHC molecules to initiate intracellular signaling that can ultimately lead to the upregulation of gene transcription factors and the activation of T cells and a concomitant immune response. In addition to these antigen-derived pMHC molecules (agonists), APC surfaces also display abundant numbers of pMHC ligands that are derived from endogenous (or self) proteins. T cells can discriminate with extraordinary sensitivity between antigen-derived and endogenous pMHC molecules, and molecular mechanisms underlying this phenomenon have been described before.[5,7,29] The molecular mechanism involves cooperative interactions between endogenous and agonist pMHC molecules in triggering TCR signaling. Furthermore, experiments and theoretical arguments have shown that endogenous pMHC molecules are recruited into the immunological synapse.[5,7,29,33] The synapse is comprised of a central cluster of TCR and pMHC molecules and a peripheral ring of adhesion molecules. The cluster of pMHC molecules includes both endogenous pMHC and agonists. We have studied the factors that influence endogenous pMHC recruitment into the immunological synapse using our algorithm.

The basic structure of the model that has been proposed for synergistic interactions between agonist and endogenous pMHC in triggering TCR signaling is as follows (Figure 2). Because of thymic selection, TCR−endogenous pMHC complexes have a very short half-life,[34] and so this interaction does not usually lead to productive downstream signaling. In contrast, TCR can bind agonists much more avidly. TCR binding to agonist pMHC molecules is sufficiently long-lived to allow the recruitment and

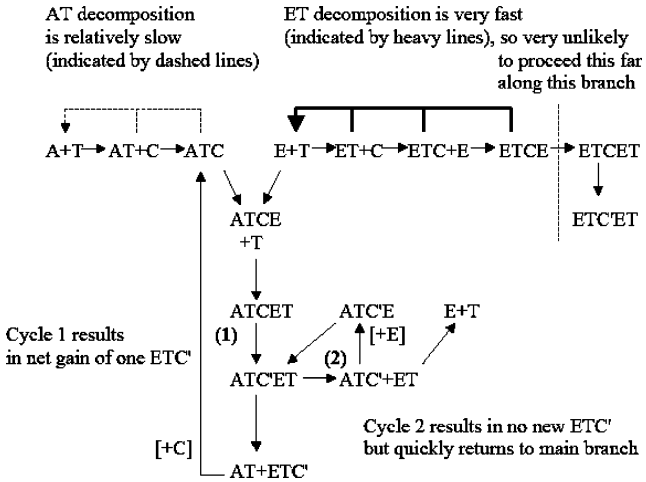

Figure 3. Further details of the reaction network simulated for studying endogenous pMHC recruitment in to the immunological synapse.

binding of the coreceptor, CD4. This coreceptor has a kinase, Lck, attached to its cytoplasmic region that can phosphorylate certain domains of the TCR complex. This phosphorylation is necessary for productive downstream signaling. While this describes why endogenous pMHCs by themselves do not trigger T cell signaling, it does not explain how signals from a few agonists are amplified. In this regard, it has been proposed that endogenous pMHC molecules are recruited to the agonist pMHC−TCR−CD4−Lck signaling complex. Although several ways have been proposed for how this may occur, the molecular details of this interaction are not understood.[5,7,29] Regardless of this molecular detail, Li et al.[7] pointed out that an enormous amplification of TCR signaling can be achieved once complexes of agonist and endogenous pMHC, TCR, and CD4 are formed. The key to the amplification mechanism is the spatial localization of the kinase Lck in this signaling complex. When a TCR binds to an endogenous pMHC molecule that is a part of complexes such as that shown in Figure 2, Lck is already spatially localized in the vicinity of TCR binding to endogenous pMHC. Thus, despite the short half-life of this interaction, Lck can phosphorylate the relevant domains and generate signaling-competent TCRs. In other words, the model suggests that agonist pMHC molecules nucleate signaling complexes (Figure 2) that convert some endogenous pMHC molecules from spectators to participants in triggering TCR.

This model is consistent with many experimental findings.[5,7] One suggestion, based on the structure of the model, is that weaker agonist pMHC molecules should result in recruiting fewer endogenous pMHC molecules into the immunological synapse. Experimental results for two different agonists (MCC88−103 and T102S) for the 5C.C.7 TCR are consistent in that the weaker agonist (T102S) results in recruitment of fewer endogenous pMHCs to the synapse. However, direct computer simulations have never been carried out to study endogenous pMHC recruitment to the synapse and its dependence on the half-life characterizing different agonists. This is because such a study requires an algorithm that can study spatially heterogeneous environments in the presence of fields responsible for synapse formation. The computational algorithm described above enables such computer simulations.

The basic signaling reactions that we simulate are shown in Figure 3 and Tables 4−6. We note one feature of the model that was not explicitly described previously[5,7,29] but appears to be necessary for describing endogenous pMHC recruitment into the synapse. When the complex shown in Figure 2d dissociates such that it contains CD4 (and associated Lck) bound to an endogenous pMHC−TCR complex, the rate at which TCR dissociates from the endogenous pMHC molecule is slower than that if CD4−Lck was not present. This stabilization is thought to be mediated by Lck binding to the TCR.[35−39]

The dynamics of the signaling reactions are coupled in our simulations to forces underlying synapse formation. Several theoretical studies have been carried out to delineate the forces involved in forming the immunological synapse. The first study was that carried out by Qi et al.[22] where they coupled equations describing binding and transport of receptors and ligands in apposing membranes to model A dynamics for the shape evolution of the T cell membrane. Further studies have followed a similar approach in studying the forces involved in synapse formation and have led to important insights.[21,23,40−43] Taken together, the basic picture that has emerged is one that was emphasized in the earliest studies.[22,24] Coupling between differential topography of various receptor−ligand pairs with cell membrane mechanics provides an underlying thermodynamic reason for segregation into spatially segregated patterns, a self-organizing tendency that is amplified and coordinated by various cellular transport and regulatory mechanisms. A transport mechanism is required for the evolution of the spatially segregated patterns which, in principle, could be due to diffusion, cytoskeletal transport, or both. In particular, as has been noted several times[3,22,24,25,43] cytoskeletal transport of TCR (triggered by early signaling events) provides a transport mechanism that amplifies segregation of receptors and ligands into the synaptic pattern. While explicitly making note of convective transport several times, for simplicity, Qi et al.[22] chose to just consider diffusion (with large values of the TCR diffusion coefficient) to illustrate the role of coupling between topographical size differences and membrane mechanics, the thermodynamic forces that underlie the emergence of spatially segregated synaptic patterns. We incorporated all the effects described in these previous studies in our simulations.

The TCR−pMHC complex that accumulates in the central supramolecular activation cluster is approximately 15 nm in size, while the complex formed upon binding of the adhesion molecules that ultimately accumulates in the peripheral supramolecular activation cluster is 42 nm. This topographic size difference couples to membrane shape. The intermembrane shape is treated as a continuous field, and the dynamic forces due to these underlying thermodynamic considerations are treated according to model A dynamics[32] as described in Appendix A. We model cytoskeletal forces triggered by TCR-based signaling as a convective bias in the diffusion of those chemical species affected by the cytoskeletal motion (e.g., TCR). Here, we follow an algorithm similar to that employed by Lee et al.,[3] albeit with a simpler signaling model. We trigger the convective bias representing cytoskeletal motion when the number of phosphorylated receptors exceeds a threshold value.

One set of simulations was performed with all of the features described above while another set of simulations of the model did not include TCR phosphorylation and the associated signaling-dependent convective transport of TCR due to cytoskeletal motion. Simulations were carried out for systems with varying off rates for the complex formed between agonist pMHC molecules and the TCR (A−T complexes). Figure 4 shows that, with the model described above, the presence of even a very small amount of agonist pMHC, with the binding kinetics characteristic of the MCC88−103 peptide presented in the $I-E^k$ context to 2B4 T cells, results in the formation of a well-defined synapse with a large number of endogenous pMHC molecules. However, in the absence of agonist, a synapse does not form.

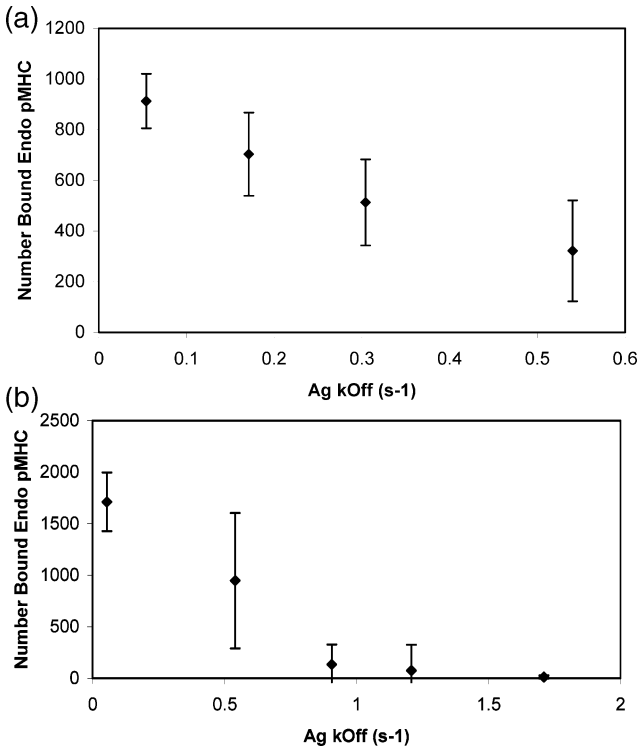

Figure 4. Fewer endogenous pMHCs are recruited in to the synapse (time $t = 600$s) as the dissociation rate (k_{off}) characterizing the binding of agonist pMHC to TCR becomes larger. The data points with the lowest value of k_{off} correspond to that for the binding of a good agonist, MCC88−103 pMHC, to the 2B4 TCR: (a) with no cytoskeletal motion; (b) with cytoskeletal motion (triggered by TCR signaling).

It is interesting to compare differences between simulations with and without cytoskeletal motion. In both cases, synapses form, but as first noted by Qi et al.[22] and subsequently by others,[21,23] directed cytoskeletal motion amplifies and coordinates synapse formation and in the present situation leads to greater levels of segregation of endogenous pMHC in the synapse.

Our simulations show that the number of endogenous pMHC−TCR complexes in the synapse depends on the agonist pMHC−TCR off rate. Figure 4 shows that there is a significant decline in the number of endogenous pMHC molecules recruited into the synapse as the agonist quality becomes weaker. This dependence is weaker (though still clearly evident) in the simulations where cytoskeletal transport triggered by TCR signaling is incorporated. These results are consistent with experimental results.[5,7] More importantly, they demonstrate that the algorithm that we have described can simulate such complex processes in a reasonable amount of computation time. Each trajectory required approximately 135 000 s (no phosphorylation or convective bias) or 725 000 s (phosphorylation and convective bias present) of wall time for simulation on AMD Athlon 2200+ MP processors.

5. Concluding Remarks

This paper presents an extension of Gillespie's First Reaction Method[18] to the case of a spatially inhomogeneous system coupled to a set of fields whose evolution is determined by PDEs (deterministic or stochastic). Such fields may arise when considering models in which the rates of the discrete reactions of the master equation are coupled to some "external" PDE (e.g., intermembrane protein complex formation rates coupling to relative motion of cell membranes), or they may arise as approximations to the dynamics of other discrete particle populations that are present in large copy numbers.

Several difficulties that appear when attempting to construct such a spatially homogeneous hybrid algorithm are discussed, and solutions are offered, including a novel stochastic clock algorithm. We compare the relative efficiency of these algorithms as well as straightforward extensions of ideas already described in the literature to model problems that contain the basic features of cell signaling processes. The algorithms that we describe perform very well. However, during the application of these solutions, it becomes apparent that the optimal method of simulation depends on certain aspects of the system under simulation. In particular, the degree to which reaction propensities are coupled (that is, the number of reaction propensities that are changed by the occurrence of a reaction event in the system) should be taken into account in deciding what method of simulation will maximize computational efficiency. Our method appears to be useful when these couplings lead to changes in many reaction propensities, a feature that may be relatively common in realistic cell signaling processes. We have illustrated the utility of our algorithm to study realistic cellular processes by showing that we can simulate a fairly complex problem relevant to the biology of T lymphocytes that was previously very difficult to accomplish.

Acknowledgment. This research was supported by the National Institutes of Health and the Defense Advanced Research Project Agency.

Appendix 1

The treatment of some species in our master equation formalism as fields as opposed to discrete populations may be understood as the replacement of particle numbers $n(\mathbf{x})$ of such species by partial averages $\langle n(\mathbf{x})\rangle/L^d = c(\mathbf{x})$, as will be described below. Here we discuss the approximations involved in this procedure (leading up to eq 12 in the text) for species that participate in reactions with only two types of kinetics. All reactions creating the species c in question must be zeroth-order in that same "field" species c (i.e., the rate of a reaction producing species c should be independent of the local concentration c, though it may depend in any way on the numbers of molecules of other species), while all reactions consuming c must be first-order in c (though again they may depend in any way on the numbers of molecules of other species). Generally speaking, we envision that c is produced in reactions of the form $a \rightarrow c + \cdots$ or $a + b \rightarrow c + \cdots$ and is consumed in reactions of the form $c \rightarrow \cdots$ or $c + d \rightarrow \cdots$, where $\cdots$ is understood not to include c.

The partial averages indicated by the brackets in the expression $c(\mathbf{x}) = \langle n(\mathbf{x})\rangle/L^d$ represent an average over fast diffusion hopping events. The times at which other discrete reactions occur are not integrated out. What we will describe here is a procedure for obtaining $c(\mathbf{x},t + \mathrm{d}t)$ given the value of $c(\mathbf{x},t)$ and the knowledge of what reaction, if any, occurred in the infinitesimal time interval $(t,t + \mathrm{d}t)$. This knowledge is obtained by following the Gillespie procedure as outlined above for the set of reactions excluding diffusion hops of c; together with the evolution equation for $c(\mathbf{x},t)$ described below, this allows us to follow the evolution of our system through all of the reaction channels available.

We consider first a species that diffuses by hopping from bin to neighboring bin on a d-dimensional lattice and that undergoes a first-order reaction removing particles with the local rate constant $r = r(\mathbf{x},t)$. Focusing on a particular bin $\mathbf{x}$, we

separate out the terms in the master equation corresponding to the reaction occurring in $\mathbf{x}$ from those terms corresponding to diffusion (anywhere) or the consumption reaction occurring at any bin $\mathbf{y} \neq \mathbf{x}$

$$\frac{\partial P(\{m\},n;t)}{\partial t} = \sum_{\{m'\},n'} [W(\{m\},n;\{m'\},n')P(\{m'\},n';t) - W(\{m'\},n';\{m\},n)P(\{m\},n;t)]$$

$$= \sum_{\{m'\},n'} [W^*(\{m\},n;\{m'\},n')P(\{m'\},n';t) - W^*(\{m'\},n';\{m\},n)P(\{m\},n;t)] + (n+1)r\,\mathrm{d}t\,P(\{m\},n+1;t) - nr\,\mathrm{d}t\,P(\{m\},n;t) \quad \text{(A1)}$$

where $n = n(\mathbf{x})$ is the number of particles in bin $\mathbf{x}$, $\{m\}$ is the set of all $n(\mathbf{y})$ for $\mathbf{y} \neq \mathbf{x}$, and W^* contains all matrix elements of the transition matrix W other than those describing the consumption reaction, which are added explicitly in the last line of eq A1. We now rewrite this equation as

$$P(\{m\},n;t+\mathrm{d}t) = P(\{m\},n;t) - nr\,\mathrm{d}t\,P(\{m\},n;t) - \sum_{\{m'\},n'} W^*(\{m'\},n';\{m\},n)P(\{m\},n;t) + \sum_{\{m'\},n'} [W^*(\{m\},n;\{m'\},n')P(\{m'\},n';t)]\,\mathrm{d}t + (n+1)r\,\mathrm{d}t P(\{m\},n+1;t) \quad \text{(A2)}$$

The terms in the first line of the right-hand side of eq A2 correspond to those trajectories starting at $(\{m\},n)$ at time t that undergo no reactions or diffusion hop in any bin $\mathbf{y}$ in the time interval $\mathrm{d}t$ (and hence are still in the state $(\{m\},n)$ at time $t + \mathrm{d}t$). The terms in the second line of eq A2 correspond to those trajectories starting at $(\{m'\},n')$ that undergo in the interval $\mathrm{d}t$ a diffusion hop (in any bin, including $\mathbf{x}$) or undergo a consumption reaction in any bin $\mathbf{y}$ *other than* $\mathbf{x}$, such that the resulting change to the system leaves it in the state $(\{m\},n)$ at time $t + \mathrm{d}t$. Finally, the third line of eq A2 corresponds to those trajectories undergoing a consumption reaction in the bin $\mathbf{x}$ carrying them to the state $(\{m\},n)$ at time $t + \mathrm{d}t$. From this discussion it should be clear that

$$P(\{m\},n;t+\mathrm{d}t \cap \text{no reaction in bin } \mathbf{x} \text{ in time } \mathrm{d}t) = P(\{m\},n;t) - nr\,\mathrm{d}t\,P(\{m\},n;t) - \sum_{\{m'\},n'} W^*(\{m'\},n';\{m\},n)P(\{m\},n;t) + \sum_{\{m'\},n'} [W^*(\{m\},n;\{m'\},n')P(\{m'\},n';t)]\,\mathrm{d}t \quad \text{(A3)}$$

and

$$P(\{m\},n;t+\mathrm{d}t \cap \text{reaction in bin } \mathbf{x} \text{ in time } \mathrm{d}t) = (n+1)r\,\mathrm{d}t\,P(\{m\},n+1;t) \quad \text{(A4)}$$

Then, invoking the definition of conditional probability, we have

$$P(\{m\},n;t+\mathrm{d}t \mid \text{no reaction in bin } \mathbf{x} \text{ in time } dt) = \frac{P(\{m\},n;t+dt \cap \text{no reaction in bin } \mathbf{x} \text{ in time } \mathrm{d}t)}{P(\text{no reaction in bin } \mathbf{x} \text{ in time } \mathrm{d}t)}$$

$$= \frac{P(\{m\},n;t) - nr\,\mathrm{d}t\,P(\{m\},n;t) - \sum_{\{m'\},n'} [W^*(\{m\},n;\{m'\},n')P(\{m'\},n';t) - W^*(\{m'\},n';\{m\},n)P(\{m\},n;t)]\,\mathrm{d}t}{\sum_{\{m\},n}(1 - nr\,\mathrm{d}t)P(\{m\},n;t)}$$

$$= \frac{P(\{m\},n;t) - nr\,\mathrm{d}t\,P(\{m\},n;t) - \sum_{\{m'\},n'} [W^*(\{m\},n;\{m'\},n')P(\{m'\},n';t) - W^*(\{m'\},n';\{m\},n)P(\{m\},n;t)]\,\mathrm{d}t}{1 - \langle n\rangle r\,\mathrm{d}t}$$

$$= P(\{m\},n;t) + \langle n\rangle r\,\mathrm{d}t - nr\,\mathrm{d}t\,P(\{m\},n;t) - \sum_{\{m'\},n'} [W^*(\{m\},n;\{m'\},n')P(\{m'\},n';t) - W^*(\{m'\},n';\{m\},n)P(\{m\},n;t)]\,\mathrm{d}t \quad \text{(A5)}$$

where in the last line we have used Taylor expansions for the denominator and ignored terms of order $(\mathrm{d}t)^2$. Similarly

$$P(\{m\},n;t+\mathrm{d}t \mid \text{reaction in bin } \mathbf{x} \text{ in time } \mathrm{d}t) = \frac{P(\{m\},n;t+\mathrm{d}t \cap \text{reaction in bin } \mathbf{x} \text{ in time } \mathrm{d}t)}{P(\text{reaction in bin } \mathbf{x} \text{ in time } \mathrm{d}t)}$$

$$= \frac{(n+1)r\,\mathrm{d}t\,P(\{m\},n+1;t)}{\sum_{\{m\},n} nr\,\mathrm{d}t\,P(\{m\},n;t)} = \frac{(n+1)r\,\mathrm{d}t\,P(\{m\},n+1;t)}{\langle n\rangle r\,\mathrm{d}t} \quad \text{(A6)}$$

We now introduce the notation

$$P_A(\{m\},n;t+\mathrm{d}t) = P(\{m\},n;t+\mathrm{d}t \mid \text{no reaction occurs in interval } \mathrm{d}t)$$

$$P_B(\{m\},n;t+\mathrm{d}t) = P(\{m\},n;t+\mathrm{d}t \mid \text{reaction occurs in interval } \mathrm{d}t) \quad \text{(A7)}$$

and indicate moments and cumulants with respect to these distributions by subscripted bracket notation (i.e., $\langle n\rangle_A$ is the average of n with respect to the distribution P_A, and $\langle\langle n^2\rangle\rangle_B$ is the variance of n with respect to the distribution P_B). Moments and cumulants with respect to the initial distribution $P(\{m\},n;t)$ will be notated by unsubscripted brackets. Thus we have

$$\begin{aligned}\langle n\rangle_A &= \sum_{\{m\},n} nP_A(\{m\},n;t+\mathrm{d}t)\\ &= \sum_{\{m\},n} n[P(\{m\},n;t) + \langle n\rangle r\,\mathrm{d}t - nr\,\mathrm{d}t\,P(\{m\},n;t) - \\ &\qquad \sum_{\{m'\},n'} [W^*(\{m\},n;\{m'\},n')P(\{m'\},n';t) - \\ &\qquad\qquad W^*(\{m'\},n';\{m\},n)P(\{m\},n;t)]\,\mathrm{d}t]\\ &= \langle n\rangle - r\,\mathrm{d}t\,\langle\langle n^2\rangle\rangle - \\ &\qquad \text{(unmodified terms from all } W^* \text{ reactions)} \end{aligned} \tag{A8}$$

and

$$\begin{aligned}\langle n\rangle_B &= \sum_{\{m\},n} nP_B(\{m\},n;t+\mathrm{d}t)\\ &= \sum_{\{m\},n} \frac{((n+1)^2 r\,\mathrm{d}t\,P(\{m\},n+1;t) - (n+1)r\,\mathrm{d}t\,P(\{m\},n+1;t))}{\langle n\rangle r\,\mathrm{d}t}\\ &= \frac{1}{\langle n\rangle}\sum_{\{m\},(n+1)} n^2P(\{m\},n;t) - nP(\{m\},n;t)\\ &= \frac{\langle n^2\rangle - \langle n\rangle}{\langle n\rangle} = \frac{\langle\langle n^2\rangle\rangle + \langle n\rangle^2 - \langle n\rangle}{\langle n\rangle}\\ &= \langle n\rangle + \frac{\langle\langle n^2\rangle\rangle}{\langle n\rangle} - 1\end{aligned} \tag{A9}$$

Thus we have equations for the average number of particles n present in bin $\mathbf{x}$ at time dt in the disjointed sets of trajectories for which either (A) no reaction occurred in the interval dt or (B) a reaction did happen in the interval dt. Note also that the influence of diffusion is uncoupled from that of the reaction, as is the influence of reactions at other bins $\mathbf{y} \neq \mathbf{x}$.

In the above, we have considered the effect of splitting our initial ensemble of trajectories into two subensembles $B = B(\mathbf{x})$ and $A = A(\mathbf{x})$ (consisting of those trajectories in which a destruction event does or does not occur in bin $\mathbf{x}$ in the time interval $(t,t+\mathrm{d}t)$) on the evolution of $n(\mathbf{x},t)$ in the same bin $\mathbf{x}$ as the potential reaction event. In Appendix 2, we show that we can ignore the effects of reactions in $\mathbf{x}$ on the populations in other bins $\mathbf{y} \neq \mathbf{x}$ when the following conditions hold:

(i) $P_i(\mathbf{y};t) \ll \Sigma_j P_j(\mathbf{y};t) = \langle n(\mathbf{y};t)\rangle$ for all particles i, bins $\mathbf{y}$, and times t. As long as there are no spatial regions in which one particular particle is very likely to be present and all others are not, this condition should be met if there are suitably many particles present in total.

(ii) $L^2/D \ll r(\mathbf{y})$, that is, the characteristic time scale for a particle to diffuse the distance of one bin length is much less than the time for a particle to be destroyed by the first-order reaction.

It should be noted that the reaction terms in eqs A8 and A9 depend only on the variance of the statistical distribution of n at the starting time t. As we seek a closed equation for the evolution of $\langle n\rangle$, it is especially useful if we can relate the variance of the distribution to its mean. In Appendix 2, we show that the relation $\langle\langle n^2\rangle\rangle = \langle n\rangle$ holds when the conditions i and ii above are satisfied. Then, eqs A8 and A9 simplify to

$$\begin{aligned}\langle n(\mathbf{x})\rangle_A &= \langle n(\mathbf{x})\rangle - \langle n(\mathbf{x})\rangle r\,\mathrm{d}t + \text{diffusion terms}\\ \langle n(\mathbf{x})\rangle_B &= \langle n(\mathbf{x})\rangle + O(\mathrm{d}t)\end{aligned} \tag{A10}$$

The second equation tells us simply that $\langle n(\mathbf{x})\rangle$ does not undergo any discontinuous change at those instants in which a reaction occurs; as dt approaches zero, the density of intervals in which a reaction occurs also goes to zero, so that the first line of eq A10 applies at all times. In the large $\langle n\rangle$ limit under which the diffusion terms cross over into Fick's law, we can rewrite the first equation above symbolically as

$$\frac{\partial\langle n(\mathbf{x})\rangle}{\partial t} = D\nabla^2\langle n(\mathbf{x})\rangle - r\langle n(\mathbf{x})\rangle \tag{A11}$$

if we understand the Laplacian in a discretized sense (and in the limit of an infinitesimal bin size it crosses over to the true Laplacian operator).

If the species of interest is not only consumed in reactions with first-order (in the species itself) kinetics but also created as a result of reactions with zeroth-order (again with respect to the particular species itself) kinetics, we require a separation of time scales between the hopping of the species from bin to bin and the first-order consumption reaction. Upon the creation of a particle by the zeroth-order reaction, say in bin $\mathbf{x}$, the expectation value $\langle n(\mathbf{x})\rangle$ is increased by 1, but the variance $\langle\langle n(\mathbf{x})^2\rangle\rangle$ is unchanged, so that we no longer have a closed equation for the evolution of $\langle n(\mathbf{x})\rangle$ (since the closed equation derived above results from the replacement of $\langle\langle n^2\rangle\rangle$ by $\langle n\rangle$). However, if we have a separation of time scales such that we can assume that the probability distribution of the spatial location of the created particle has time to spread out over many bins before it has any chance of being consumed by the first-order consumption reaction, we can argue as in Appendix 2 that $n(\mathbf{x})$ will still be Poisson-distributed. Thus, in this approximation we may still use eq A11 to describe the evolution of $\langle n(\mathbf{x})\rangle$, though we must now include the zeroth-order reaction term

$$\frac{\partial\langle n(\mathbf{x})\rangle}{\partial t} = D\nabla^2\langle n(\mathbf{x})\rangle - r\langle n(\mathbf{x})\rangle + \sum_i \delta(t - t_i(\mathbf{x})) \tag{A12}$$

where $\{t_i(\mathbf{x})\}$ is the statistically distributed set of times when the zeroth-order creation reaction occurs in bin $\mathbf{x}$. Setting $c(\mathbf{x};t) = \langle n(\mathbf{x};t)\rangle L^{-d}$, where L is the side length of one bin, we see that the above is the spatial discretization of the PDE

$$\frac{\partial c(\mathbf{x})}{\partial t} = D\nabla^2 c(\mathbf{x}) - rc(\mathbf{x}) + \sum_{\mathbf{x}'}\delta(\mathbf{x}-\mathbf{x}')\sum_i \delta(t - t_i(\mathbf{x}')) \tag{A13}$$

where the summation over $\mathbf{x}'$ is taken over the discrete locations of all of the bins in the system still used in describing the state of the remaining discrete variables.

Allowing the rate constant for the first-order destruction process to vary in space and time does not alter the considerations leading to this approximation—in fact, this rate constant may even depend on the local populations of species other than

the one(s) treated as fields without essentially altering the arguments above. Thus a second-order reaction that is first-order in the "field" species and first-order also in a (different) nonfield species may be considered for the purposes of these approximations as a first-order destruction reaction for the field species with a spatially and temporally varying rate constant equal to the second-order rate constant times the local population of the nonfield species in question. Similarly, any reaction that produces a field species but whose kinetics are zeroth-order in the field species (though of any order with respect to the discretely treated species) can be considered for the purposes of the field equation to be a zeroth-order reaction with a spatially varying rate constant. In this situation we are led to the equation

$$\frac{\partial c(\mathbf{x},t)}{\partial t} = D\nabla^2 c(\mathbf{x},t) - k(\mathbf{x},t)c(\mathbf{x},t) + \sum_{\mathbf{x}'} \delta(\mathbf{x}-\mathbf{x}')S \sum_j \delta(t - t_j(\mathbf{x}')) \quad \text{(A14)}$$

where $k(\mathbf{x},t)$ is the spatially (and temporally) varying rate constant for the reaction consuming the species represented by c and $\{t_j(\mathbf{x})\}$ is the statistically distributed set of times for the reaction producing S particles of the species represented by c at $\mathbf{x}$. Finally, if there are m total reactions, we write

$$\frac{\partial c(\mathbf{x},t)}{\partial t} = D\nabla^2 c(\mathbf{x},t) - \sum_{i=1}^{m} k_i(\mathbf{x},t)c(\mathbf{x},t) + \sum_{i=1}^{m}\sum_{\mathbf{x}'} \delta(\mathbf{x}-\mathbf{x}')S_i \sum_j \delta(t - t_{i,j}(\mathbf{x}')) \quad \text{(A15)}$$

where $k_i(\mathbf{x},t) = 0$ for those reactions that do not consume species c and $S_i = 0$ for those reactions that do not produce species c.

Appendix 2

In this appendix we first show that we can ignore the effects of reactions in $\mathbf{x}$ on the populations in other bins $\mathbf{y} \neq \mathbf{x}$. Let $P_i(\mathbf{x})$ denote the probability that the ith particle is in bin $\mathbf{x}$. We demonstrate below that, as long as only zeroth-order creation processes and first-order destruction processes are present, $P_i(\mathbf{x})$ will be independent of $P_j(\mathbf{x})$ where i and j are not equal.

We consider the changes to the statistical distributions of particle number in bin $\mathbf{y}$ as a result of splitting into subensembles $A = A(\mathbf{x})$ and $B = B(\mathbf{x})$ based on the occurrence, or lack thereof, of a reaction in bin $\mathbf{x}$. Then (here we do not explicitly include the diffusion terms in the equation for the evolution of $P_i(\mathbf{y};t)$, since to the first order in dt, they are independent of the reaction terms)

$$\begin{aligned} P_i(\mathbf{y};t+\mathrm{d}t \mid \text{no reaction at } \mathbf{x}) &= \frac{P_i(\mathbf{y};t+\mathrm{d}t \cap \text{no reaction at } \mathbf{x})}{P(\text{no reaction at } \mathbf{x})} \\ &= \frac{[P_i(\mathbf{y};t)(1-r(\mathbf{y})\,\mathrm{d}t)][1-\sum_{j\neq i} r(\mathbf{x})\,\mathrm{d}t\,P_j(\mathbf{x};t)]}{1-r(\mathbf{x})\,\mathrm{d}t\,\langle n(\mathbf{x})\rangle} \\ &= \frac{[P_i(\mathbf{y};t)(1-r(\mathbf{y})\,\mathrm{d}t)][1-r(\mathbf{x})\,\mathrm{d}t\langle n(\mathbf{x})\rangle + r(\mathbf{x})\,\mathrm{d}tP_i(\mathbf{x};t)]}{1-r(\mathbf{x})\,\mathrm{d}t\,\langle n(\mathbf{x})\rangle} \\ &= P_i(\mathbf{y};t) - r(\mathbf{y})\,\mathrm{d}t\,P_i(\mathbf{y};t) + r(\mathbf{x})\,\mathrm{d}tP_i(\mathbf{y};t)P_i(\mathbf{x};t) \end{aligned} \quad \text{(A16)}$$

In Appendix 1, the subensemble $A(\mathbf{x})$ is defined to contain trajectories in which no reaction occurs in bin $\mathbf{x}$ in the time interval $(t,t+\mathrm{d}t)$; thus we can rewrite the result above as

$$P_{i,A(\mathbf{x})}(\mathbf{y};t+\mathrm{d}t) = P_i(\mathbf{y};t) - r(\mathbf{y})\,\mathrm{d}t\,P_i(\mathbf{y};t) + r(\mathbf{x})\,\mathrm{d}t\,P_i(\mathbf{y};t)P_i(\mathbf{x};t) \quad \text{(A17)}$$

while for the subensemble $B(\mathbf{x})$ defined to contain those trajectories in which a reaction does occur in bin $\mathbf{x}$ in the interval $(t,t+\mathrm{d}t)$

$$\begin{aligned} P_{i,B(\mathbf{x})}(\mathbf{y};t+\mathbf{d}t) &= \frac{P_i(\mathbf{y};t+\mathrm{d}t \cap \text{reaction at } \mathbf{x})}{P(\text{reaction at } \mathbf{x})} \\ &= \frac{[P_i(\mathbf{y};t)(1-r(\mathbf{y})\,\mathrm{d}t)]\left[\sum_{j\neq i} r(\mathbf{x})\,\mathrm{d}t\,P_j(\mathbf{x};t)\right]}{r(\mathbf{x})\,\mathrm{d}t\,\langle n(\mathbf{x})\rangle} \\ &= \frac{[P_i(\mathbf{y};t)(1-r(\mathbf{y})\,\mathrm{d}t)]r(\mathbf{x})\,\mathrm{d}t[\langle n(\mathbf{x})\rangle - P_i(\mathbf{x};t)]}{r(\mathbf{x})\,\mathrm{d}t\,\langle n(\mathbf{x})\rangle} \\ &= P_i(\mathbf{y};t) - r(\mathbf{y})\,\mathrm{d}t\,P_i(\mathbf{y};t) - \frac{P_i(\mathbf{y};t)P_i(\mathbf{x};t)}{\langle n(\mathbf{x})\rangle} + \frac{r(\mathbf{y})\,\mathrm{d}t\,P_i(\mathbf{y};t)P_i(\mathbf{x};t)}{\langle n(\mathbf{x})\rangle} \end{aligned} \quad \text{(A18)}$$

However, our real interest is to split the trajectories into subensembles $B(\{\mathbf{x}\})$ consisting of those trajectories in which a reaction happened in the set of bins $\{\mathbf{x}\}$ and no reaction occurred in those bins not in the set $\{\mathbf{x}\}$. We assume that the probability that any given particle is destroyed in dt is small, so that the number of particles that are destroyed is small compared to the total number and that the contribution of any one particle to the expected value of particles in bin $\mathbf{y}$ is small (i.e., $P_i(\mathbf{y};t) \ll \sum P_j(\mathbf{y};t) = \langle n(\mathbf{y})\rangle$). Then, we obtain the following expression for the probability that a reaction occurs in the bin $\mathbf{y}$ given that particles $\{1,2,...,i\}$ have been destroyed in bins

$\{\mathbf{x}_1,\mathbf{x}_2,...,\mathbf{x}_i\}$and that no particles were destroyed in any bins $\mathbf{z} \notin \{\mathbf{x}\}$, $\mathbf{z} \neq \mathbf{y}$ during the interval dt

$$P(\text{reaction at } \mathbf{y} \text{ in } (t,t+\mathrm{d}t)|\{i\} \text{ destroyed in } \{\mathbf{x}_i\} \cap \text{no other reactions})$$

$$= \frac{P(\text{reaction at } \mathbf{y} \text{ in } (t,t+\mathrm{d}t) \cap \{i\} \text{ destroyed in } \{\mathbf{x}_i\} \cap \text{no other reactions})}{P(\{i\} \text{ destroyed in } \{\mathbf{x}_i\} \cap \text{no other reactions})}$$

$$= \sum_{j=i+1}^{N} \frac{P(j\text{th particle destroyed in bin } \mathbf{y} \cap \{i\} \text{ destroyed in } \{\mathbf{x}_i\} \cap \text{no other particles destroyed})}{\left[\prod_{k=1}^{i} P_k(\mathbf{x}_k;t)r(\mathbf{x}_k)\,\mathrm{d}t\right]\left[1-\sum_{j=i+1}^{N}\sum_{\mathbf{z}\notin\{\mathbf{x}\},\mathbf{z}\neq\mathbf{y}} P_j(\mathbf{z};t)r(\mathbf{z})\,\mathrm{d}t\right]}$$

$$= \frac{\left[\prod_{k=1}^{i} P_k(\mathbf{x}_k;t)r(\mathbf{x}_k)\,\mathrm{d}t\right]\sum_{j=i+1}^{N} \frac{P_j(\mathbf{y};t)}{1-\sum_{l=i+1,l\neq j}^{N}\sum_{\mathbf{z}} P_l(\mathbf{z};t)r(\mathbf{z})\,\mathrm{d}t} r(\mathbf{y})\,\mathrm{d}t}{\left[\prod_{k=1}^{i} P_k(\mathbf{x}_k;t)r(\mathbf{x}_k)\,\mathrm{d}t\right]\left[1-\sum_{j=i+1}^{N}\sum_{\mathbf{z}\notin\{\mathbf{x}\},\mathbf{z}\neq\mathbf{y}} P_j(\mathbf{z};t)r(\mathbf{z})\,\mathrm{d}t\right]}$$

$$= \frac{\sum_{j=i+1}^{N}[P_j(\mathbf{y};t)r(\mathbf{y})\,\mathrm{d}t + O(\mathrm{d}t^2)]}{1-\sum_{j=i+1}^{N}\sum_{\mathbf{z}\notin\{\mathbf{x}\},\mathbf{z}\neq\mathbf{y}} P_j(\mathbf{z};t)r(\mathbf{z})\,\mathrm{d}t}$$

$$= \sum_{j=i+1}^{N} P_j(\mathbf{y};t)r(\mathbf{y})\,\mathrm{d}t + O(\mathrm{d}t^2)$$

$$= \sum_{j=1}^{N} P_j(\mathbf{y};t)r(\mathbf{y})\,\mathrm{d}t - \sum_{j=1}^{i} P_j(\mathbf{y};t)r(\mathbf{y})\,\mathrm{d}t$$

$$\approx \sum_{j=1}^{N} P_j(\mathbf{y};t)r(\mathbf{y})\,\mathrm{d}t = \langle n(\mathbf{y})\rangle r(\mathbf{y})\,\mathrm{d}t$$

$$= P(\text{reaction at } \mathbf{y} \text{ in } (t,t+\mathrm{d}t)) \qquad \text{(A19)}$$

In other words, to the first order in dt and with the approximation $P_i(\mathbf{y};t) \ll \langle n(\mathbf{y})\rangle$, the probability of a reaction occurring in bin $\mathbf{y}$ in interval dt is independent of the occurrence or not of reactions in any other bins.

The manipulations immediately above concern the likelihood of a reaction occurring in bin $\mathbf{y}$. We now return to the probability that particle i will be in bin $\mathbf{y}$ given reactions in bins $\{\mathbf{x}\}$, $P_{i,B(\{\mathbf{x}\})}(\mathbf{y};t+\mathrm{d}t)$. To this end, note also that with the condition $P_i(\mathbf{y};t) \ll \langle n(\mathbf{y})\rangle$, the last term in eq A18 derived for $P_{i,B(\mathbf{x})}(\mathbf{y};t+\mathrm{d}t)$ above, can be ignored, as it contains the product of two small quantities, dt and $P_i/\langle n\rangle$. Then (we repeat the equation for $P_{i,A(\mathbf{x})}(\mathbf{y};t+\mathrm{d}t)$ below as well for convenience)

$$P_{i,B(\mathbf{x})}(\mathbf{y};t+\mathrm{d}t) = P_i(\mathbf{y};t) - r(\mathbf{y})\,\mathrm{d}tP_i(\mathbf{y};t) - \frac{P_i(\mathbf{y};t)P_i(\mathbf{x};t)}{\langle n(\mathbf{x})\rangle}$$

$$P_{i,A(\mathbf{x})}(\mathbf{y};t+\mathrm{d}t) = P_i(\mathbf{y};t) - r(\mathbf{y})\,\mathrm{d}t\,P_i(\mathbf{y};t) + r(\mathbf{x})\,\mathrm{d}t\,P_i(\mathbf{y};t)P_i(\mathbf{x};t) \qquad \text{(A20)}$$

Rewriting

$$P_{i,B(\mathbf{x})}(\mathbf{y};t+\mathrm{d}t) = P_{i,\text{common}}(\mathbf{y};t+\mathrm{d}t) + \Delta P_{i,B(\mathbf{x})}(\mathbf{y};t+\mathrm{d}t)$$

$$P_{i,A(\mathbf{x})}(\mathbf{y};t+\mathrm{d}t) = P_{i,\text{common}}(\mathbf{y};t+\mathrm{d}t) + \Delta P_{i,A(\mathbf{x})}(\mathbf{y};t+\mathrm{d}t) \qquad \text{(A21)}$$

where

$$P_{i,\text{common}}(\mathbf{y};t) = P_i(\mathbf{y};t) - r(\mathbf{y})\,\mathrm{d}t\,P_i(\mathbf{y};t)$$

$$\Delta P_{i,B(\mathbf{x})}(\mathbf{y};t+\mathrm{d}t) = -\frac{P_i(\mathbf{y};t)P_i(\mathbf{x};t)}{\langle n(\mathbf{x})\rangle} \qquad \text{(A22)}$$

$$\Delta P_{i,A(\mathbf{x})}(\mathbf{y};t+\mathrm{d}t) = r(\mathbf{x})\,\mathrm{d}t\,P_i(\mathbf{y};t)P_i(\mathbf{x};t)$$

Note also that $P_{i,\text{common}}(\mathbf{y};t) = P(i \text{ in } \mathbf{y} \text{ at } t+\mathrm{d}t)$; i.e., $P_{i,\text{common}}(\mathbf{y};t)$ is equal to the probability that the ith particle is in bin $\mathbf{y}$ at time $t+\mathrm{d}t$ given no information about what reactions have or have not occurred elsewhere in the system.

Denoting the event that a reaction occurs at $\mathbf{x}$ by $r_{\mathbf{x}}$ and that a reaction does not occur at $\mathbf{x}$ by $s_{\mathbf{x}}$

$$P_{i,B(\{\mathbf{x}\})}(\mathbf{y};t+\mathrm{d}t) = P(i\text{th particle in bin } \mathbf{y} \text{ at } t+\mathrm{d}t \mid \text{reactions at } \{\mathbf{x}\} \cap \text{no reactions at } \mathbf{z}\notin\{\mathbf{x}\})$$

$$= \frac{P(i\text{th particle in bin } \mathbf{y} \text{ at } t+\mathrm{d}t \cap \text{reactions at } \{\mathbf{x}\} \cap \text{no reactions at } \mathbf{z}\notin\{\mathbf{x}\})}{P(\text{reactions at } \{\mathbf{x}\} \cap \text{no reactions at } \mathbf{z}\notin\{\mathbf{x}\})}$$

$$= P(i \text{ in } \mathbf{y} \text{ at } t+\mathrm{d}t) \times \frac{\left[\prod_{\mathbf{z}\in\{\mathbf{x}\}} P(r_{\mathbf{z}}|i \text{ in } \mathbf{y} \text{ at } t+\mathrm{d}t)\right]\left[\prod_{\mathbf{z}\in\{\mathbf{x}\}} P(s_{\mathbf{z}}|i \text{ in } \mathbf{y} \text{ at } t+\mathrm{d}t)\right]}{\prod_{\mathbf{z}\notin\{\mathbf{x}\}} P(r_{\mathbf{z}}) \prod_{\mathbf{z}\notin\{\mathbf{x}\}} P(s_{\mathbf{z}})} \qquad \text{(A23)}$$

In going from line 2 to line 3 of eq A23 above, we have used, in the denominator, the independence of the events $r_{\mathbf{z}}$ and $s_{\mathbf{z}}$ derived above, while in the numerator we have used the *conditional* independence of the events $r_{\mathbf{z}}$ and $s_{\mathbf{z}}$ given the event

i in $\mathbf{y}$ at $t + \mathrm{d}t$. By this we mean that

$$P(r_{\mathbf{z}}|i \text{ in } \mathbf{y} \text{ at } t + \mathrm{d}t \cap r_{\mathbf{x}_1} \cap r_{\mathbf{x}_2} \cap \cdots \cap r_{\mathbf{x}_a} \cap s_{\mathbf{y}_1} \cap s_{\mathbf{y}_2} \cap \cdots \cap s_{\mathbf{y}_b}) = P(r_{\mathbf{z}}|i \text{ in } \mathbf{y} \text{ at } t + \mathrm{d}t)$$

$$P(s_{\mathbf{z}}|i \text{ in } \mathbf{y} \text{ at } t + \mathrm{d}t \cap r_{\mathbf{x}_1} \cap r_{\mathbf{x}_2} \cap \cdots \cap r_{\mathbf{x}_a} \cap s_{\mathbf{y}_1} \cap s_{\mathbf{y}_2} \cap \cdots \cap s_{\mathbf{y}_b}) = P(s_{\mathbf{z}}|i \text{ in } \mathbf{y} \text{ at } t + \mathrm{d}t) \quad \text{(A24)}$$

for all $\{\mathbf{x}_j\}$ and $\{\mathbf{y}_k\}$ such that $\mathbf{z}$ is not a member of either set. This conditional independence can be verified by a calculation analogous to that of eq A19. Continuing with the calculation of $P_{i,B(\{\mathbf{x}\})}(\mathbf{y};t + \mathrm{d}t)$, we now invoke Baye's formula to simplify eq A23

$$P_{i,B(\{\mathbf{x}\})}(\mathbf{y};t + \mathrm{d}t) = P(i \text{ in } \mathbf{y} \text{ at } t + \mathrm{d}t) \times \left[\prod_{\mathbf{z}\in\{\mathbf{x}\}} \frac{P(i \text{ in } \mathbf{y} \text{ at } t + \mathrm{d}t|r_{\mathbf{z}})P(r_{\mathbf{z}})}{P(i \text{ in } \mathbf{y} \text{ at } t + \mathrm{d}t)}\right] \times \frac{\left[\prod_{\mathbf{z}\in\{\mathbf{x}\}} \frac{P(i \text{ in } \mathbf{y} \text{ at } t + \mathrm{d}t|s_{\mathbf{z}})P(s_{\mathbf{z}})}{P(i \text{ in } \mathbf{y} \text{ at } t + \mathrm{d}t)}\right]}{\left[\prod_{\mathbf{z}\in\{\mathbf{x}\}} P(r_{\mathbf{z}})\right]\left[\prod_{\mathbf{z}\notin\{\mathbf{x}\}} P(s_{\mathbf{z}})\right]}$$

$$= P(i \text{ in } \mathbf{y} \text{ at } t + \mathrm{d}t) \times \left[\prod_{\mathbf{z}\in\{\mathbf{x}\}} \frac{P(i \text{ in } \mathbf{y} \text{ at } t + \mathrm{d}t|r_{\mathbf{z}})}{P(i \text{ in } \mathbf{y} \text{ at } t + \mathrm{d}t)}\right]\left[\prod_{\mathbf{z}\in\{\mathbf{x}\}} \frac{P(i \text{ in } \mathbf{y} \text{ at } t + \mathrm{d}t|s_{\mathbf{z}})}{P(i \text{ in } \mathbf{y} \text{ at } t + \mathrm{d}t)}\right]$$

$$= P_{i,\mathrm{common}}(\mathbf{y};t + \mathrm{d}t) \times \left[\prod_{\mathbf{z}\in\{\mathbf{x}\}} \frac{P_{i,B(\mathbf{z})}(\mathbf{y};t + \mathrm{d}t)}{P_{i,\mathrm{common}}(\mathbf{y};t + \mathrm{d}t)}\right]\left[\prod_{\mathbf{z}\notin\{\mathbf{x}\}} \frac{P_{i,A(\mathbf{z})}(\mathbf{y};t + \mathrm{d}t)}{P_{i,\mathrm{common}}(\mathbf{y};t + \mathrm{d}t)}\right]$$

$$= P_{i,\mathrm{common}}(\mathbf{y};t + \mathrm{d}t) \times \left[\prod_{\mathbf{z}\in\{\mathbf{x}\}} \left(1 + \frac{\Delta P_{i,B(\mathbf{z})}(\mathbf{y};t + t\,\mathrm{d}t)}{P_{i,\mathrm{common}}(\mathbf{y};t + \mathrm{d}t)}\right)\right]\left[\prod_{\mathbf{z}\notin\{\mathbf{x}\}} \left(1 + \frac{\Delta P_{i,A(\mathbf{z})}(\mathbf{y};t + t\,\mathrm{d}t)}{P_{i,\mathrm{common}}(\mathbf{y};t + \mathrm{d}t)}\right)\right]$$

$$= P_{i,\mathrm{common}}(\mathbf{y};t + \mathrm{d}t) + \sum_{\mathbf{z}\notin\{\mathbf{x}\}} \Delta P_{i,A(\mathbf{z})}(\mathbf{y};t + \mathrm{d}t) + \sum_{\mathbf{z}\in\{\mathbf{x}\}} \Delta P_{i,B(\mathbf{z})}(\mathbf{y};t + \mathrm{d}t) + O(\Delta P^2) \quad \text{(A25)}$$

Now substituting back in the values for $P_{i,\mathrm{common}}$ and ΔP_i, we have

$$P_{i,B(\{\mathbf{x}\})}(\mathbf{y};t + \mathrm{d}t) = P_i(\mathbf{y};t) - r(\mathbf{y})\,\mathrm{d}t\,P_i(\mathbf{y};t) + \sum_{\mathbf{z}\notin\{\mathbf{x}\}} r(\mathbf{z})\,\mathrm{d}t\,P_i(\mathbf{y};t)P_i(\mathbf{z};t) - \sum_{\mathbf{z}\in\{\mathbf{x}\}} \frac{P_i(\mathrm{y};t)P_i(\mathbf{z};t)}{\langle n(\mathbf{z})\rangle}$$

$$= P_i(\mathbf{y};t) - r(\mathbf{y})\,\mathrm{d}t\,P_i(\mathbf{y};t) + \sum_{\mathbf{z}} r(\mathbf{z})\,\mathrm{d}t\,P_i(\mathrm{y};t)P_i(\mathbf{z};t) - \sum_{\mathbf{z}\in\{\mathbf{x}\}} \frac{P_i(\mathbf{y};t)P_i(\mathbf{z};t)}{\langle n(\mathbf{z})\rangle} - \sum_{\mathbf{z}\in\{\mathbf{x}\}} r(\mathbf{z})\,\mathrm{d}t\,P_i(\mathbf{y};t)P_i(\mathbf{z};t) \quad \text{(A26)}$$

Noting that the number of bins in the set $\{\mathbf{x}\}$ undergoing reactions in the interval $\mathrm{d}t$ is $O(N\,\mathrm{d}t)$ where N is the total number of bins in the system, we see that the last term in eq A26 above is $O(\mathrm{d}t^2)$ and hence negligible. Then

$$P_{i,B(\{\mathbf{x}\})}(\mathbf{y};t + \mathrm{d}t) = P_i(\mathbf{y};t) - r(\mathbf{y})\,\mathrm{d}t\,P_i(\mathbf{y};t) + \sum_{\mathbf{z}} r(\mathbf{z})\,\mathrm{d}t\,P_i(\mathbf{y};t)P_i(\mathbf{z};t) - \sum_{\mathbf{z}\in\{\mathbf{x}\}} \frac{P_i(\mathbf{y};t)P_i(\mathbf{z};t)}{\langle n(\mathbf{z})\rangle}$$

$$= P_i(\mathbf{y};t) - r(\mathbf{y})\,\mathrm{d}t\,P_i(\mathbf{y};t) + P_i(\mathbf{y};t)\left[\sum_{\mathbf{z}} r(\mathbf{z})\,\mathrm{d}t\,P_i(\mathbf{z};t) - \sum_{\mathbf{z}\in\{\mathbf{x}\}} \frac{P_i(\mathbf{z};t)}{\langle n(\mathbf{z})\rangle}\right] \quad \text{(A27)}$$

We now show that the quantity in brackets vanishes in the appropriate limit, justifying the neglect of effects on reactions in bins $\mathbf{x} \neq \mathbf{y}$ on the populations in bin $\mathbf{y}$. Given that each bin $\mathbf{z}$ undergoes a reaction in $\mathrm{d}t$ with probability $\langle n(\mathbf{z})\rangle r(\mathbf{z})\,\mathrm{d}t$, we see that the expectation value over the statistical distribution of sets $\{\mathbf{x}\}$ of bins undergoing reactions of the term in brackets is given by

$$\left\langle \sum_{\mathbf{z}} r(\mathbf{z})\,\mathrm{d}t\,P_i(\mathbf{z};t) - \sum_{\mathbf{z}\in\{\mathbf{x}\}} \frac{P_i(\mathbf{z};t)}{\langle n(\mathbf{z})\rangle}\right\rangle_{P(\{\mathbf{x}\})} = \sum_{\mathbf{z}} r(\mathbf{z})\,\mathrm{d}t\,P_i(\mathbf{z};t) - \sum_{\mathbf{z}} \left\langle \frac{P_i(\mathbf{z};t)}{\langle n(\mathbf{z})\rangle}\right\rangle_{P(\mathbf{z} \text{ undergoes reaction})}$$

$$= \sum_{\mathbf{z}} \left(r(\mathbf{z})\,\mathrm{d}t\,P_i(\mathbf{z};t) - \frac{P_i(\mathbf{z};t)}{\langle n(\mathbf{z})\rangle} P(\mathbf{z} \text{ undergoes reaction})\right)$$

$$= \sum_{\mathbf{z}} P_i(\mathbf{z};t)\left(r(\mathbf{z})\,\mathrm{d}t - \frac{1}{\langle n(\mathbf{z})\rangle}\langle n(\mathbf{z})\rangle r(\mathbf{z})\,\mathrm{d}t\right)$$

$$= \sum_{\mathbf{z}} P_i(\mathbf{z};t)(r(\mathbf{z})\,\mathrm{d}t - r(\mathbf{z})\,\mathrm{d}t) = 0 \quad \text{(A28)}$$

We consider also the variance

$$\left\langle\left\langle\left(\sum_{\mathbf{z}} r(\mathbf{z})\,\mathrm{d}t\,P_i(\mathbf{z};t) - \sum_{\mathbf{z}\in\{\mathbf{x}\}} \frac{P_i(\mathbf{z};t)}{\langle n(\mathbf{z})\rangle}\right)^2\right\rangle\right\rangle_{P(\{\mathbf{x}\})} = \sum_{\mathbf{z}} \left\langle\left\langle\left(\frac{P_i(\mathbf{z};t)}{\langle n(\mathbf{z})\rangle}\right)^2\right\rangle\right\rangle_{P(\mathbf{x} \text{ undergoes reaction})}$$

$$= \sum_{\mathbf{z}} \left(\frac{P_i(\mathbf{z};t)}{\langle n(\mathbf{z})\rangle}\right)^2 P(\mathbf{x} \text{ undergoes reaction})$$

$$= \sum_{\mathbf{z}} \frac{P_i(\mathbf{z};t)^2}{\langle n(\mathbf{z})\rangle^2}\langle n(\mathbf{z})\rangle r(\mathbf{z})\,\mathrm{d}t$$

$$= \mathrm{d}t \sum_{\mathbf{z}} \frac{r(\mathbf{z})P_i(\mathbf{z};t)^2}{\langle n(\mathbf{z})\rangle} \quad \text{(A29)}$$

If the variance is negligible, then we are justified in replacing the bracketed term in eq A27 with its average, which we have just shown vanishes. Thus we are interested in the conditions under which the expression $\sum_{\mathbf{z}} r(\mathbf{z})P_i(\mathbf{z};t)^2/\langle n(\mathbf{z})\rangle$ is negligible. Physically, a combination of fast diffusion on the length scale L of one bin (so that the probability distribution $P_i(\mathbf{z};t)$ spreads out rapidly enough that $P_i(\mathbf{z};t) \ll 1$ is valid for all $\mathbf{z}$ and t) and high average particle number $\langle n(\mathbf{z})\rangle \gg 1$ in every bin $\mathbf{z}$ will result in the quantity in question being small (we do also assume

that $r(\mathbf{z})$ is bounded). Then we can write

$$P_{i,B(\{\mathbf{x}\})}(\mathbf{y};t + \mathrm{d}t) = P_i(\mathbf{y};t)(1 - r(\mathbf{y})\,\mathrm{d}t) \tag{A30}$$

It is in this limit that we can ignore the effects of reactions in bin $\mathbf{x}$ on the populations in other bins $\mathbf{y}$.

We now show that in the appropriate limit the statistical distribution $P_{\mathbf{x},t}(n)$ for the number of particles in bin $\mathbf{x}$ at time t is Poissonian. Defining the variables $n_i(\mathbf{x},t)$ by $n_i(\mathbf{x},t) = 1$ if the ith particle is in bin $\mathbf{x}$ at time t and $n_i(\mathbf{x},t) = 0$ otherwise, we see that $P(n_i(\mathbf{x},t) = 1) = P_i(\mathbf{x};t)$, where $P_i(\mathbf{x};t)$ is again the probability that the ith particle is in bin $\mathbf{x}$ at time t and as well

$$n(\mathbf{x};t) = \sum_i n_i(\mathbf{x};t) \tag{A31}$$

If, for all i, $P_i(\mathbf{x}) \ll 1$ (that is, the probability distribution for the location of particle i is spread out over many bins such that the likelihood it is in any specific bin $\mathbf{x}$ is very small), then we will have (remembering also that the stochastic variables n_i defined above are independent as long as all creation processes are zeroth-order in $n = \Sigma\, n_i$ and destruction processes first order in n)

$$\begin{aligned}\langle\langle n^k(\mathbf{x})\rangle\rangle &= \sum_i \langle\langle n_i^k(\mathbf{x})\rangle\rangle \\ &= \sum_i 1^k P_i(\mathbf{x}) + O(P_i(\mathbf{x})^2) \\ &= \sum_i P_i(\mathbf{x})\end{aligned} \tag{A32}$$

where $\langle\langle n^k\rangle\rangle$ denotes the kth cumulant of the distribution of n. Thus cumulants of all orders exist and are equal for the distribution. This is true also of Poisson distributions and in fact is sufficient to prove that the distribution $P_{\mathbf{x},t}(n)$ is a Poisson distribution.

We have just shown that $\langle\langle n(\mathbf{x})^2\rangle\rangle = \langle n(\mathbf{x})\rangle$, and thus, returning to eqs A8 and A9 of Appendix 1, we can now say

$$\begin{aligned}\langle n(\mathbf{x})\rangle_A &= \langle n(\mathbf{x})\rangle - \langle n(\mathbf{x})\rangle r\,\mathrm{d}t + \text{diffusion terms} \\ \langle n(\mathbf{x})\rangle_B &= \langle n(\mathbf{x})\rangle + O(\mathrm{d}t)\end{aligned} \tag{A33}$$

Appendix 3: Treatment of the Membrane Field

The membrane forces are treated by representing the intermembrane separation as a field evolving according a to a time-dependent Landau−Ginzburg formalism (model A dynamics[32])

$$\frac{\partial z(x,y,t)}{\partial t} = -M\frac{\delta F}{\delta z(x,y,t)} + \xi \tag{A34}$$

where ξ is a white noise term and the free energy functional is given by

$$F[z] = \int \frac{1}{2}[\gamma(\nabla z)^2 + \kappa(\nabla^2 z)^2 + \sum_i \lambda_i c_i(x,y)(z(x,y) - z_i)^2]\,\mathrm{d}x\,\mathrm{d}y \tag{A35}$$

where in the last term i ranges over all molecules binding across the gap between the two membranes, λ_i, z_i are the appropriate parameters for species i, and c_i is the local concentration of species i (or, in the case of discrete species, we interpret c_i as n_i, the number of molecules in the bin corresponding to location (x,y)).

Those reactions that produce intermembrane species (i.e., complexes binding across the gap between cells) have a membrane-dependent reaction rate constant given by

$$k_i(z) = k_{i,0}\left[1 - H\left(\frac{|z - z_i|}{\chi_i}\right)\right]\exp\left[-\frac{(z - z_i)^2}{2\sigma_i^2}\right] \tag{A36}$$

where $k_{i,0}$ is the base rate constant, H is the Heaviside step function, z_i is the height (i.e., the preferred binding distance for the complex produced by reaction i), σ_i is the interaction range, and χ_i is the cutoff for reaction i.

The diffusion of intermembrane species i is also subject to the addition of a convective term resulting from the membrane separation field, with a velocity given by

$$v_i^M = \frac{D_i}{k_B T}\nabla\frac{\delta F}{\delta c_i} \tag{A37}$$

with the added constraint that diffusion of intermembrane species i in regions for which $|z - z_i| > \chi_i$ is prohibited.

Values of the membrane parameters used (ref 43 and references therein) were

$$\begin{aligned}\gamma &= 28.125kT\,\mu\mathrm{m}^{-2} \\ \kappa &= 15kT \\ M &= 0.00004(kT)^{-1}\,\mu\mathrm{m}^2\,\mathrm{s}^{-1}\end{aligned}$$

References and Notes

(1) Alberts, B.; Johnson, A.; Lewis, J.; Raff, M.; Roberts, K.; Walter, P. *Molecular Biology of the Cell*, 4th ed.; Garland Publishing: New York, 2002.
(2) Bunnell, S. C.; Barr, V. A.; Fuller, C. L.; Samelson, L. E. *Sci. STKE* **2003**, PL8.
(3) Lee, K. H.; Dinner, A. R.; Tu, C.; Campi, G.; Raychaudhuri, S.; Varma, R.; Sims, T. N.; Burack, W. R.; Wu, H.; Wang, J.; Kanagawa, O.; Markiewicz, M.; Allen, P. M.; Dustin, M. L.; Chakraborty, A. K.; Shaw, A. S. *Science* **2003**, *302*, 1218.
(4) Lee, K.-H.; Holdorf, A. D.; Dustin, M. L.; Chan, A. C.; Allen, P. M.; Shaw, A. S. *Science* **2002**, *295*, 1539.
(5) Krogsgaard, M.; Li, Q.-J.; Sumen, C.; Huppa, J. B.; Huse, M.; Davis, M. M. *Nature* **2005**, *434*, 238.
(6) Grakoui, A.; Bromley, S. K.; Sumen, C.; Davis, M. M.; Shaw, A. S.; Allen, P. M.; Dustin, M. L. *Science* **1999**, *285*, 221.
(7) Li, Q.-J.; Dinner, A. R.; Qi, S.; Irvine, D. J.; Huppa, J. B.; Davis, M. M.; Chakraborty, A. K. *Nat. Immunol.* **2004**, *5*, 791.
(8) Monks, C. R. F.; Freiberg, B. A.; Kupfer, H.; Sciaky, N.; Kupfer, A. *Nature* **1998**, *395*, 82.
(9) Huppa, J. B.; Davis, M. M. *Nat. Rev. Immunol.* **2003**, *3*, 973.
(10) Morrison, D. K.; Davis, R. J. *Annu. Rev. Cell Dev. Biol.* **2003**, *19*, 91.
(11) Lipkow, K.; Andrews, S. S.; Bray, D. *J. Bacteriol.* **2005**, *187*, 45.
(12) Sachs, K.; Perez, O.; Pe'er, D.; Lauffenburger, D. A.; Nolan, G. P. *Science* **2005**, *308*, 523.
(13) Coombs, D.; Kalergis, A. M.; Nathenson, S. G.; Wofsy, C.; Goldstein, B. *Nat. Immunol.* **2002**, *3*, 926.
(14) Goldstein, B.; Faeder, J. R.; Hlavacek, W. S. *Nat. Rev. Immunol.* **2004**, *4*, 445.
(15) Van Kampen, N. G. *Stochastic Processes in Physics and Chemistry*; Elsevier: New York, 2001.
(16) Frenkel, D.; Smith, B. *Understanding Molecular Simulation: From Algorithms to Applications*; Elsevier: San Diego, 1996.
(17) Chan, C.; George, A. J. T.; Stark, J. *Proc. Natl. Acad. Sci. U.S.A.* **2001**, *98*, 5758.
(18) Gillespie, D. T. *J. Phys. Chem.* **1977**, *81*, 2340.
(19) Elf, J.; Doncic, A.; Ehrenberg, M. *Proc. SPIE−Int. Soc. Opt. Eng.* **2003**, *5110*, 114.
(20) Raychaudhuri, S.; Chakraborty, A. K.; Kardar, M. *Phys. Rev. Lett.* **2003**, *91*, 208101.
(21) Weikl, T. R.; Lipowsky, R. *Biophys. J.* **2004**, *87*, 3665.
(22) Qi, S. Y.; Groves, J. T.; Chakraborty, A. K. *Proc. Natl. Acad. Sci. U.S.A.* **2001**, *98*, 6548.
(23) Burroughs, N. J.; Wulfing, C. *Biophys. J.* **2002**, *83*, 1784.
(24) Chakraborty, A. K. *Sci. STKE* **2002**, PE10.

(25) Wulfing, C.; Davis, M. M. *Science* **1998**, *282*, 2266.
(26) Takahashi, K.; Kaizu, K.; Hu, B.; Tomita, M. *Bioinformatics* **2004**, *20*, 538.
(27) Salis, H.; Kaznessis, Y. N. *J. Chem. Phys.* **2005**, *122*, 054103.
(28) Gibson, M. A.; Bruck, J. *J. Phys. Chem. A* **2000**, *104*, 1876.
(29) Irvine, D. J.; Purbhoo, M. A.; Krogsgaard, M.; Davis, M. M. *Nature* **2002**, *419*, 845.
(30) Bortz, A. B.; Kalos, M. H.; Leibowitz, J. L. *J. Comput. Phys.* **1975**, *17*, 10.
(31) Newman, M. E. J.; Barekma, G. T. *Monte Carlo Methods in Statistical Physics*; Oxford University Press: Oxford, U. K., 1999.
(32) Hohenberg, P. C.; Halperin, B. I. *Rev. Mod. Phys.* **1977**, *49*, 435.
(33) Wulfing, C.; Sumen, C.; Sjaastad, M. D.; Wu, L. C.; Dustin, M. L.; Davis, M. M. *Nat. Immunol.* **2002**, *3*, 42.
(34) Janeway, C. A.; Travers, P.; Walport, M.; Schlomchik, M. J. *Immunobiology: The Immune System in Health and Disease*, 6th ed.; Garland Science Publishing: New York, 2005.
(35) Collins, T. L.; Uniyal, S.; Shin, J.; Strominger, J. L.; Mittler, R. S.; Burakoff, S. J. *J. Immunol.* **1992**, *148*, 2159.
(36) Rivas, A.; Takada, S.; Koide, J.; Sonderstrup-McDevitt, G.; Engleman, E. G. *J. Immunol.* **1988**, *140*, 2912.
(37) Rudd, C. E.; Anderson, P.; Morimoto, C.; Streuli, M.; Schlossman, S. F. *Immunol. Rev.* **1989**, *111*, 225.
(38) Janeway, C. A. *Annu. Rev. Immunol.* **1992**, *10*, 645.
(39) Vignali, D. A.; Doyle, C.; Kinch, M. S.; Shin, J.; Strominger, J. L. *Philos. Trans. R. Soc. London, Ser. B* **1993**, *342*, 13.
(40) Chen, H.-J. *Phys. Rev. E* **2003**, *67*, 031919.
(41) Coombs, D.; Dembo, M.; Wofsy, C.; Goldstein, B. *Biophys. J.* **2004**, *86*, 1408.
(42) Weikl, T. R.; Groves, J. T.; Lipowsky, R. *Europhys. Lett.* **2002**, *59*, 916.
(43) Lee, S. J.; Hori, Y.; Groves, J. T.; Dustin, M. L.; Chakraborty, A. K. *Trends Immunol.* **2002**, *23*, 500.